(12) INTERNATIONAL APPLICATION PUBLISHED UNDER THE PATENT COOPERATION TREATY (PCT)

(19) World Intellectual Property Organization
International Bureau

(43) International Publication Date
6 May 2004 (06.05.2004)

PCT

(10) International Publication Number
WO 2004/037088 A1

(51) International Patent Classification[7]: A61B 6/03, 6/00

(21) International Application Number:
PCT/IB2003/004457

(22) International Filing Date: 9 October 2003 (09.10.2003)

(25) Filing Language: English

(26) Publication Language: English

(30) Priority Data:
10/280,734 25 October 2002 (25.10.2002) US

(71) Applicant: KONINKLIJKE PHILIPS ELECTRONICS N.V. [NL/NL]; Groenewoudseweg 1, NL-5621 BA Eindhoven (NL).

(71) Applicant *(for AE only)*: U.S. PHILIPS CORPORATION [US/US]; 1251 Avenue of the Americas, New York, NY 10510-8001 (US).

(72) Inventor: HEUSCHER, Dominic, J.; 595 Miner Road, Cleveland, OH 44143 (US).

(74) Common Representative: KONINKLIJKE PHILIPS ELECTRONICS N.V.; c/o LUNDIN, Thomas, M., 595 Miner Road, Cleveland, OH 44143 (US).

(81) Designated States *(national)*: AE, AG, AL, AM, AT, AU, AZ, BA, BB, BG, BR, BY, BZ, CA, CH, CN, CO, CR, CU, CZ, DE, DK, DM, DZ, EC, EE, ES, FI, GB, GD, GE, GH, GM, HR, HU, ID, IL, IN, IS, JP, KE, KG, KP, KR, KZ, LC, LK, LR, LS, LT, LU, LV, MA, MD, MG, MK, MN, MW, MX, MZ, NI, NO, NZ, OM, PH, PL, PT, RO, RU, SC, SD, SE, SG, SK, SL, TJ, TM, TN, TR, TT, TZ, UA, UG, UZ, VC, VN, YU, ZA, ZM, ZW.

(84) Designated States *(regional)*: ARIPO patent (GH, GM, KE, LS, MW, MZ, SD, SL, SZ, TZ, UG, ZM, ZW), Eurasian patent (AM, AZ, BY, KG, KZ, MD, RU, TJ, TM), European patent (AT, BE, BG, CH, CY, CZ, DE, DK, EE, ES, FI, FR, GB, GR, HU, IE, IT, LU, MC, NL, PT, RO, SE, SI, SK, TR), OAPI patent (BF, BJ, CF, CG, CI, CM, GA, GN, GQ, GW, ML, MR, NE, SN, TD, TG).

Published:
— *with international search report*

For two-letter codes and other abbreviations, refer to the "Guidance Notes on Codes and Abbreviations" appearing at the beginning of each regular issue of the PCT Gazette.

(54) Title: FOUR-DIMENSIONAL HELICAL TOMOGRAPHIC SCANNER

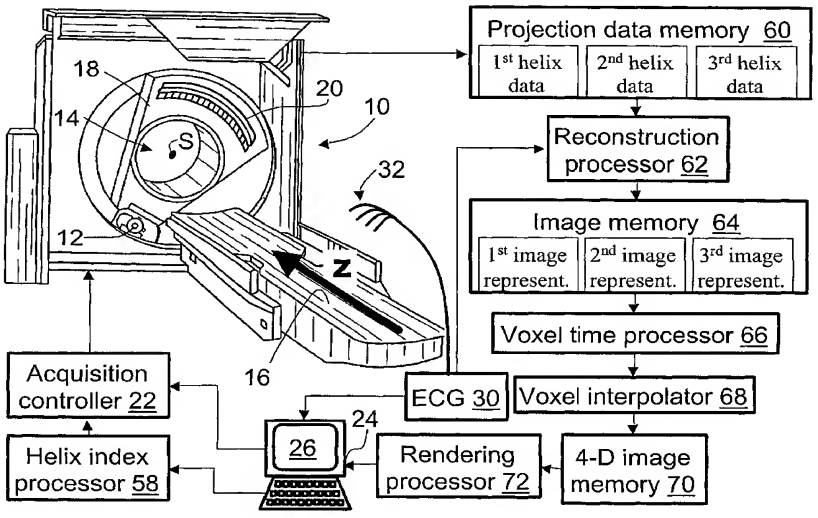

(57) Abstract: A computed tomography imaging scanner (10) acquires helical cone beam projection data for a volume of interest (46) using at least two source trajectory helices. A reconstruction processor (62) reconstructs the projection data for each helix to generate a corresponding time skewed image representation. A voxel time processor (66) computes an acquisition time for each voxel in each time skewed image representation. A voxel interpolator (68) computes an interpolated voxel value for each voxel based on values of the voxel in the time skewed image representations and corresponding voxel acquisition times. In an electronic embodiment, the computed tomography scanner (10) includes an x ray source (12) with an axially oriented cylindrical anode (92), an electron source (961, 962) irradiating the cylindrical anode (92) to produce an x ray beam (120, 122, 124, 126), and an electron beam deflector (98, 100) that deflects the electron beam along the anode (92) to axially sweep the x ray beam.

WO 2004/037088 A1

FOUR-DIMENSIONAL HELICAL TOMOGRAPHIC SCANNER

The present invention relates to the medical imaging arts. It particularly relates to high-speed and time-dependent helical or multi-slice volumetric cardiac computed tomography (CT) imaging, and will be described with particular reference thereto. However, the invention will also find application in volumetric computed tomographic imaging of other dynamically moving organs, in high resolution contrast agent intake and blood perfusion studies, and the like.

Cardiac computed tomography imaging typically employs an x-ray source that generates a fan-beam, wedge-beam, cone-beam or otherwise-shaped beam of x-rays that traverse an examination region within which a patient's heart is disposed. The cardiac tissue, coronary arteries, and blood interacts with and absorbs a portion of the traversing x-rays. Typically, a contrast agent is administered to the patient to improve blood contrast. A one- or two-dimensional radiation detector arranged opposite the x-ray source detects and measures intensities of the transmitted x-rays.

During scanning the patient is linearly advanced between axial scans to perform multi-slice computed tomography imaging, or the patient is continuously linearly advanced during x-ray source rotation to perform helical computed tomography imaging. The imaging data is reconstructed using a filtered backprojection, a PI reconstruction, or the like to generate volumetric image representations. Preferably, the cardiac cycle is monitored by an electrocardiograph or other device, and the imaging data is binned into cardiac phase bins to reconstruct the heart at a plurality of phases.

A wide range of cardiac studies are performed using cardiac computed tomography imaging. Qualitative review of cardiac computed tomography images by trained medical personnel detects congenital heart defects, large aneurysms or stenoses in the major coronary arteries, and other gross anatomical abnormalities. Analyses such as heart pumping capacity

measurements, blood perfusion studies in coronary tissues, and coronary vessel tracking provide complementary quantitative diagnostic information.

In cardiac imaging, problems arise due to a limited temporal resolution of computed tomography, which is controlled by the rotation rate of the x-ray source. To reduce image artifacts, imaging data over at least a half-rotation of the x-ray source (i.e., 180° of data) is preferably acquired for each voxel. At presently achievable gantry rotation rates which are limited by x-ray flux, mechanical stability, and other factors, acquisition of a half-rotation of projection data requires about a tenth of a second or longer. Since the cardiac cycle spans about one second, substantial motion blurring is typically observed.

In cardiac cycle gating, imaging data is acquired using a circular or low-pitch spiral radiation source trajectory such that each voxel remains in the field of view over two or more cardiac cycles. Simultaneously acquired electrocardiographic data is used to select computed tomographic projection data from two or more cardiac cycles that approximately correspond to a selected cardiac phase. The selected data are combined to form a complete data set of about 180° or more for each voxel, and this combined data set is reconstructed to produce an image representation of that cardiac phase.

However, data combined from adjacent cardiac cycles may not readily form a complete data set due to angular redundancies. Synchronizing the rotation with the cardiac cycle to ensure angularly complementary data typically results in sub-optimal computed tomography imaging parameters, for example a reduced gantry rotation rate. Moreover the cardiac cycle can vary during image acquisition, especially in subjects with coronary disease or other cardiac malfunctions.

Another source of error with cardiac gating is inaccuracy in associating the electrocardiographic data with the cardiac cycle. It is known in the art that cardiac motion is only approximately related to the electrocardiographic

signal, and that physical motion cycles of the heart components vary non-linearly with variations in the cardiac cycle period, and moreover vary from subject to subject. Particularly in cases of heart arrhythmia where the cardiac cycle period is sometimes variable over a few neighboring heart beats, simple linear scaling of cardiac cycle features with cardiac cycle period is of limited accuracy.

Yet another problem with cardiac gating is that for large volume fields of view the low-pitch spiral takes a substantial length of time to span the volume of interest. This can produce artifacts due to subject motion that vary in an unknown manner along the axial direction. Alternatively, a large-area beam and corresponding large-area detector can be employed to enable use of a larger spiral pitch. However, this increases system cost, and image artifacts can occur due to spatial non-uniformity of the large-area beam or detector.

The present invention contemplates an improved apparatus and method that overcomes the aforementioned limitations and others.

According to one aspect of the invention, a helical cone beam computed tomography imaging method is provided. Helical cone beam computed tomography projection data is acquired for a volume of interest using a plurality of source trajectory helices. The acquired helical cone beam computed tomography projection data for each helix are reconstructed to generate a corresponding time skewed volume image representation of the volume of interest. For each time skewed volume image representation, a voxel acquisition time is computed for each voxel. For each voxel, an interpolated voxel value is computed based on values of the voxel in the plurality of image representations and corresponding voxel acquisition times.

According to another aspect of the invention, an apparatus is disclosed for performing helical cone beam computed tomography imaging. A means is provided for acquiring

helical cone beam computed tomography projection data for a volume of interest using a plurality of source trajectory helices. A means is provided for reconstructing the acquired helical cone beam computed tomography projection data for each helix to generate a corresponding time skewed volume image representation of the volume of interest. A means is provided for computing a voxel acquisition time for each voxel of each time skewed image representation. A means is provided for computing an interpolated voxel value for each voxel based on values of the voxel in the plurality of time skewed image representations and corresponding voxel acquisition times.

According to yet another aspect of the invention, an x-ray tube is disclosed, including a cylindrical anode whose cylindrical axis is axially oriented. An electron source produces an electron beam generally directed toward the cylindrical anode. The electron beam interacts with the cylindrical anode to produce x-rays. An electron beam deflector sweeps the electron beam axially across the cylindrical anode.

One advantage of the present invention resides in increased reconstruction accuracy compared with conventional cardiac gating employing circular or low-pitch spiral orbits. The improved accuracy is particularly apparent for large volumes of interest.

Another advantage of the present invention resides in improved temporal resolution at the voxel level.

Yet another advantage of the present invention resides in reduced sensitivity to heart arrhythmia through the use of a large-pitch spiral source trajectory that substantially spans the volume of interest in about one cardiac cycle period or less.

Numerous additional advantages and benefits of the present invention will become apparent to those of ordinary skill in the art upon reading the following detailed description of the preferred embodiment.

The invention may take form in various components and arrangements of components, and in various process operations and arrangements of process operations. The drawings are only for the purpose of illustrating preferred embodiments and are not to be construed as limiting the invention.

FIGURE 1 shows an exemplary four-dimensional helical computed tomography imaging apparatus for performing four-dimensional cardiac imaging.

FIGURE 2 shows an exemplary three interlaced helical trajectories generated by cyclic relative axial motion of the x-ray tube and the volume of interest.

FIGURE 3A shows a cardiac phase-axial position map of projection data acquired using ten helices initiated at evenly spaced cardiac percentage phase intervals, and interpolative constructing of ten cardiac phase image representations therefrom.

FIGURE 3B shows a cardiac phase-axial position map of projection data acquired using ten helices initiated at cardiac percentage phase intervals adjusted to compensate for variations in the heart rate such that a constructed slice at z=50 is sampled at substantially uniformly spaced cardiac phases.

FIGURE 3C shows a cardiac phase-axial position map of projection data acquired using ten helices initiated at cardiac percentage phase intervals adjusted to compensate for variations in the heart rate to improve a constructed 70% cardiac phase.

FIGURE 3D shows a cardiac phase-axial position map of projection data acquired using five helices each initiated at a 40% cardiac percentage phase with starting axial positions selected to particularly target imaging of a 70% cardiac phase over an axial interval $[z_{low}, z_{high}]$.

FIGURE 3E shows a cardiac phase-axial position map of projection data acquired using twelve helices each initiated at

a 40% cardiac percentage phase, the helices being performed in a bi-directional or back-and-forth fashion.

FIGURE 4 shows an exemplary a helical trajectory produced by two x-ray beams spaced 360° apart, generated using a plurality of x-ray tubes, a multi-anode x-ray tube, or an axially extended-anode x-ray tube.

FIGURE 5A shows a preferred embodiment of an x-ray tube that provides for electronic axial sweeping of an x-ray beam and/or axial switching between a plurality of axially spaced x-ray beams.

FIGURE 5B shows a suitable x-ray beam collimation arrangement for four axially spaced x-ray beams produced by the x-ray tube of FIGURE 5A.

FIGURE 6A shows first helical half-turns acquired during a first 180° gantry rotation using switched x-ray beams that are axially swept across the cylindrical anode of the x-ray tube of FIGURES 5A and 5B.

FIGURE 6B shows second helical half-turns acquired during a second 180° gantry rotation following the first 180° gantry rotation of FIGURE 5A.

FIGURE 7 plots the x-ray position on the anode for an arbitrary one of the electron beams of FIGURES 6A and 6B relative to an initial position of the beam. A corresponding arrangement of the anode and the volume of interest for the labeled gantry angles is schematically illustrated below each gantry angle label.

FIGURE 8A shows a map of projection data acquisition time versus axial position for sampling performed using the electronically switched/swept x-ray beam embodiment of FIGURES 5-7.

FIGURE 8B shows a map of projection data acquisition time versus axial position for sampling performed in alternating axial directions using the electronically switched/swept x-ray beam embodiment of FIGURES 5-7.

With reference to FIGURE 1, a computed tomography (CT) imaging scanner **10** includes an x-ray source **12** that produces a fan-shaped, cone-shaped, wedge-shaped, or otherwise-shaped x-ray beam directed into an examination region **14** which contains an imaging subject (not shown) arranged on a subject support **16**. For cardiac imaging, a patient is positioned with the subject heart substantially centered within the examination region **14**. The subject support **16** is linearly movable in a **Z**-direction while the x-ray source **12** is mounted on a rotating gantry **18** that rotates around the **Z**-axis.

In a mechanical computed tomography imaging embodiment, the rotating gantry **18** rotates simultaneously with linear advancement of the subject support **16** to produce a generally helical trajectory of the x-ray source **12** about the examination region **14**. In an electronic operating embodiment, the subject support **16** remains stationary and the x-ray source **12** electronically sweeps the x-ray beam axially across the examination region **14** during gantry rotation. The x-ray source **12** preferably produces a wedge- or cone-shaped x-ray beam that diverges in the imaging plane and in the Z-direction.

An x-ray detector **20** is arranged on the gantry **18** across from the x-ray source **12**. The x-ray detector **20** preferably includes several rows of detectors along the **Z**-direction for simultaneously acquiring imaging data along a portion of the **Z**-direction in each projection view. The x-ray detector **20** is arranged on the rotating gantry **18** opposite to the x-ray source **12** and rotates therewith so that the x-ray detector **20** receives x-rays that traverse the examination region **14** as the rotating gantry **18** rotates. Instead of the arrangement shown in FIGURE 1, it is also contemplated to

arrange the x-ray detector on a stationary gantry encircling the rotating gantry such that the x-rays continuously impinge upon a continuously shifting angular portion of the radiation detector during x-ray source rotation.

A computed tomography imaging data acquisition controller **22** controls the scanner **10** to perform selected imaging operations using helical trajectories of the x-ray source **12** relative to the subject. The helical trajectories can be accomplished by gantry rotation in cooperation with relative mechanical axial motion of the x-ray tube **12** and the subject support **16**, or by gantry rotation in cooperation with electronic axial motion of the x-ray beam. A user interface device **24**, which is typically a personal computer, workstation, or other computer device, communicates with the acquisition controller **22** to allow a user to construct, select, initiate, monitor, or otherwise supervise a selected imaging session. The user interface device **24** preferably includes a graphical display **26**.

In cardiac computed tomography imaging, a contrast agent is preferably administered to the patient to selectively improve x-ray contrast of the blood. For steady state studies, the contrast agent is preferably administered as an intravenous drip at a steady state rate to provide a generally steady state x-ray contrast for cardiac computed tomography imaging. For perfusion studies or contrast agent intake studies, a bolus injection of the contrast agent is administered, in which a substantial quantity of contrast agent is rapidly intravenously injected. In some types of cardiac imaging, the contrast agent is optionally omitted.

Cardiac computed tomography imaging also typically employs a device for monitoring the cardiac cycle. This device is typically an electrocardiograph (ECG) **30**, although an ultrasonic imaging device or other device can also be used. As

is known in the art, the electrocardiograph **30** includes a plurality of electrical leads **32** that contact the subject's chest to detect electrical signals associated with the cardiac cycle.

Although cardiac imaging is particularly described herein, it should be appreciated that the imaging can pertain to other types of cyclical temporal variations in a patient or other subject. Moreover, the imaging can pertain to non-cyclical temporal variations in the subject, such as contrast agent intake studies.

With continuing reference to FIGURE 1 and with further reference to FIGURE 2, in a mechanical embodiment of four-dimensional helical computed tomographic imaging, the acquisition controller **22** performs a plurality of large-pitch helical scans or source trajectories **40, 42, 44** that quickly cover a volume of interest **46** defined by an imaging subject such as a heart. For convenience in computing various imaging parameters, a cylindrical volume of interest **46** having a central cylindrical axis **48** is shown. In a suitable mechanical embodiment, the plurality of source trajectories **40, 42, 44** are acquired by moving the subject volume of interest **46** on the subject support **16** back and forth a selected distance **D** along the axial or **Z**-direction while the gantry **18** and x-ray source **12** rotate. For cardiac imaging, each source trajectory helix **40, 42, 44** preferably covers the cardiac volume of interest **46** in a time interval that is less than about one cardiac cycle in length.

The first helix **40** is generated by relative movement of the source **12** and the volume of interest **46** in a **+Z**-direction. The source trajectory helix **40** initiates at a starting point **50** and terminates at a point **52**.

The second helix **42** initiates at the point **52** at the same angular coordinate as the first trajectory helix **40**

terminated at. However, the second helix **42** is generated by relative movement of the source **12** and the volume of interest **46** in a **-Z**-direction. The second helix **42** terminates at a point **54**.

The third helix **44** initiates at the point **54** at the same angular coordinate as the second trajectory helix **42** terminated at. The third helix **44** is generated by relative movement of the source **12** and the volume of interest **46** in a **+Z**-direction. The third trajectory **44** terminates at a point **56**.

Optionally, additional trajectories can be generated by continuing the back and forth relative axial motion of the source **12** and the volume of interest **46**. It will also be appreciated that only two trajectories can be employed. Furthermore, it will be appreciated that in an alternative embodiment, the scans can all occur in the same direction, for example in the **+Z**-direction, with the subject support **16** returning to its initial position before each scan in the **+Z**-direction.

Moreover, although the helices **40, 42, 44** are temporally continuous, that is, each helical trajectory starts substantially immediately upon termination of the previous trajectory, it is also contemplated to include a delay between helices. For example, initiation of each trajectory helix is optionally triggered by a selected signal from the electrocardiograph **30** such that the plurality of helices span the cardiac cycle.

Preferably, each helix **40, 42, 44** is acquired in one cardiac cycle period or less. For a cardiac volume of interest **46** such as a heart which is typically about twelve centimeters along the axial or **Z**-direction, the helical trajectories **40, 42, 44** are large-pitch helical trajectories. The x-ray source **12** produces a conical- or wedge-shaped beam which is collimated to have a divergence in the axial or **Z**-direction and a helical

source trajectory pitch such that for each trajectory **40**, **42**, **44** each voxel in the volume of interest **46** remains within the field of view for about 180° or more of angular rotation of the source **12**. This provides sufficient angular data to accurately reconstruct the voxel.

With particular reference returning to FIGURE 1, a helix index processor **58** communicates with the acquisition controller **22** to specify and index the several helices **40**, **42**, **44**. A projection data memory **60** stores projection data of the first, second, and third helices **40**, **42**, **44** in corresponding data bins. A reconstruction processor **62** reconstructs projection data of each of the helices **40**, **42**, **44** to produce corresponding image representations that are stored in an image memory **64**. As discussed below, each of the image representations reconstructed from one of the helices **40**, **42**, **44** is time skewed since projection data for voxels axially located near the end of the helix are acquired later than projection data for voxels axially located near the beginning of the helix.

Each image voxel of each image representation is acquired from angularly contiguous projection data acquired over an angular interval during which the voxel remains within the field of view. For a helical pitch selected such that a voxel located on the central cylindrical axis **48** remains in the field of view for an angular interval of 180°, the angular viewing interval for a voxel lying a distance R away from the central axis **48** lies within a range of angular intervals bounded by:

$$\Delta\theta_{r,\theta,z} = \pi \pm \sin^{-1}\left(\frac{R}{S}\right) \qquad (1),$$

where S is a distance between the radiation source **12** and an isocenter **S** of the examination region **14** and $\Delta\theta_{r,\theta,z}$ is the maximum and minimum angular interval (for the "+" and "−"

options, respectively, of the "±" operator) during which the voxel at R remains in the field of view. For example, for R=15 cm and S=57 cm, $\Delta\theta_{r,\theta,z}$ is in the range of 164° to 195°.

The angular interval bounds $\Delta\theta_{r,\theta,z}$ correspond to temporal viewing interval bounds, that is, temporal resolution bounds, given by:

$$\text{Temporal resolution} = \frac{T_{rot} \cdot \Delta\theta_{r,\theta,z}}{2\pi} \qquad (2),$$

where T_{rot} is the time period for a 360° rotation of the x-ray source **12**. For R=15 cm and S=57 cm, and T_{rot}=0.4 sec (rotation rate = 150 rpm) the temporal resolution of each voxel lies in a range of 0.183 sec to 0.217 sec.

Although the equation (2) gives bounds for the temporal resolution of each voxel of the image representations that are stored in an image memory **64**, the overall image is acquired over a substantially longer period. For example, in FIGURE 2 each trajectory **40**, **42**, **44** spans about 850° and is therefore acquired (for T_{rot}=0.4 sec) over about 0.95 sec. The three scans collectively are acquired over about 2.8 sec. As a result, there is a substantial time skew of the voxels making up the image representations.

With continuing reference to FIGURES 1 and 2, to account for the time skew a voxel time processor **66** computes a voxel acquisition time for each voxel. In a preferred embodiment, this computation is based on the PI-line corresponding to each voxel. As is known in the art, the PI-line intersects the voxel and the two nearest points along the corresponding helical trajectory **40**, **42**, **44**. These two nearest points are designated herein as angles θ_1 and θ_2 (where the beginning of the scan is taken as θ=0° and the scan progresses in a positive angular direction). Since the voxel is

reconstructed from projection data acquired during the contiguous angular interval $[\theta_1, \theta_2]$ corresponding to a contiguous temporal interval, an average or mean angle θ_{avg} at which the projection data for the voxel was acquired is given by:

$$\theta_{avg} = \frac{\theta_1 + \theta_2}{2} \qquad (3).$$

The mean angle θ_{avg} corresponds to a mean or average time for the voxel acquisition given by:

$$\text{Voxel time} = \frac{T_{rot} \cdot \theta_{avg}}{2\pi} + T_o \qquad (4),$$

where T_o is the time for $\theta=0°$, that is, the time when the helical trajectory was initiated. The voxel acquisition time given by equations (3) and (4) is preferably computed by the voxel time processor **66**.

A substantial time skew exists between slices along the axial or **Z**-direction. However, even within an axial slice the voxels will be time skewed and have differing voxel acquisition times due to differences in the contiguous angular interval $[\theta_1, \theta_2]$ of the corresponding PI lines. It will be recognized that the contiguous angular viewing intervals $[\theta_1, \theta_2]$ for the voxels are determined by the reconstruction processor **62** as part of the usual cone beam image reconstruction process.

In addition to a voxel acquisition time, each voxel also has a value, such as a gray scale intensity value, in each of the time skewed image representations. As each such voxel value was acquired at about the corresponding voxel acquisition time, a time-dependent voxel value is readily computed using interpolation, curve fitting, or another method by a voxel

interpolator **68**. The time-dependent voxel values for the voxels comprising the volume of interest **46** define a four-dimensional image representation over the volume of interest **46** and the acquisition interval of the several trajectories **40**, **42**, **44**. The four-dimensional image representation is stored in a four-dimensional image memory **70**.

Alternatively, an image of the volume of interest **46** at a selected time is generated by selecting voxels whose voxel acquisition time corresponds to the selected time. Preferably, two or more voxel values with voxel acquisition times near the selected time are interpolated, curve-fitted, or otherwise combined by the voxel interpolator **68** to estimate the value of the voxel at the selected time. By performing such interpolation for each voxel in the volume of interest **46**, an image representation corresponding to the selected time with improved temporal resolution is obtained.

The four-dimensional image representation or the image representation at the selected time is preferably processed by a rendering processor **72** which produces a three-dimensional rendering for the selected time, image projections or slices at the selected time, a temporal sequence of image projections or slices, a cinematic (CINE) sequence for the imaged volume over the imaging interval, or the like, which is displayed on the graphical display **26** of the user interface device **24**.

For cardiac imaging, each helical trajectory or scan is preferably gated based on the cardiac cycling information provided by the electrocardiograph **30** to sample all cardiac cycle phases of interest. If each helix is initiated at a different phase of the cardiac cycle, for example by gating initiation of each trajectory, then for N scans a corresponding N cardiac phases can be reconstructed. The value N is given by:

$$N = \frac{T_{cc}}{0.25 \cdot T_{rot}} = \frac{240}{HR \cdot T_{rot}} \quad (5)$$

where T_{rot} is the time period for a 360° rotation of the x-ray source **12** in seconds, T_{cc} is the cardiac cycle period in seconds, and HR is the heart rate in beats per minute.

For example, if HR=60 beats per minute and T_{rot}=0.4 sec (radiation source rotation rate = 150 rpm) then N=10. That is, if ten trajectories or scans are acquired each starting at a different cardiac phase, then ten cardiac phases can be resolved.

With continuing reference to FIGURE 2, the helical trajectories **40**, **42**, **44** are acquired using a cyclical axial mechanical movement of one of the subject support and the radiation source. In this mechanical embodiment, and for presently achievable fields of view and source rotation rates, imaging a volume of interest **46** that extends axially about twelve centimeters, such as a heart, typically requires about a second or longer. Correspondingly, anatomical motions should exceed about one second to be tracked.

By employing cardiac gating, however, cyclical cardiac motions can be tracked by acquiring a number of helix scans corresponding to the number of cardiac phases to be resolved. The images corresponding to the several helix scans are optionally relatively spatially registered using nominally stationary image features such as the chest walls, to correct for patient motion or other motion artifacts on time scales of around the helical scan time.

A cardiac phase or state of motion is selected, and voxels of the time skewed image representations whose acquisition times are close to occurrences of the selected cardiac phase or state of motion are identified based on the cardiac cycling information provided by the electrocardiograph

30. Optionally, a physiological model of the cardiac motion is used to more precisely identify a time occurrence of the selected state of cardiac motion from the electrocardiographic data. The identified voxels are temporally interpolated, averaged, or otherwise combined to compute an image representation of the selected cardiac phase or state of motion which spans the volume of interest. Such an image representation can be computed from the time skewed image representations for each resolvable cardiac phase.

For example, with reference to FIGURE 3A a cardiac phase-axial position map of projection data acquired using ten helices initiated at evenly spaced cardiac percentage phase intervals is simulated. Helices are successively initiated at axial position z=0 via cardiac gating at each of 0%, 10%, 20%, 30%, 40%, 50%, 60%, 70%, 80%, and 90% of the cardiac cycle. The initiation of each scan is represented by a filled circle.

The acquired projection data are represented by slanted lines extending from the initiation times. The slanted lines represent the progression of cardiac phase as the helical trajectory simultaneously progresses along the axial or z-direction. A time skewed image representation is reconstructed using projection data acquired during each of the ten helices, and interpolated voxels are selectively computed for each of the ten cardiac percentage phases 0%, 10%, 20%, 30%, 40%, 50%, 60%, 70%, 80%, and 90%. Such interpolation is performed throughout the volume of interest, and the resultant interpolated images of the cardiac phases 0% (equivalent to 100%), 10%, 20%, 30%, 40%, 50%, 60%, 70%, 80%, and 90% are represented by horizontal dotted lines in FIGURE 3A.

As seen in FIGURE 3A, there is some non-uniformity in the available data for each selected cardiac phase due to heart rate variations occurring during the acquisition time of the ten helices. For example, a region **80** has widely spaced

sampling. Variations in the heart rate manifest in FIGURE 3A as variations in the slopes of the slanted lines representing the acquired projection data.

With reference to FIGURE 3B, the cardiac gating is adjusted to compensate for changes in the heart rate detected by the electrocardiograph **30**, with the objective of obtaining imaging data at uniform cardiac percentage phase intervals for an axial slice at z=50 (represented by a dark vertical line at z=50). It will be seen in FIGURE 3B that the projection view samples at z=50 are substantially uniformly spaced in cardiac phase.

With reference to FIGURE 3C, the cardiac gating is adjusted to compensate for changes in the heart rate, with the objective of obtaining spatially uniform sampling at a cardiac state near the 70% cardiac phase. The cardiac state of interest is represented by a solid generally horizontal curved line **82**. The cardiac state **82** can be, for example, a state of minimum cardiac motion, which minimum occurs at somewhat different cardiac phases for along the axial or Z-direction. Similar adjacent phases are indicated by dotted generally horizontal curved lines **84** and can also be reconstructed.

With reference to FIGURE 3D, imaging of a cardiac state **86** near the 70% cardiac phase over a range $[z_{low}, z_{high}]$ is performed. Each helix is started at a percentage cardiac phase of 40%, and projection data is acquired between 40% and 100% cardiac phase. Preferably, the x-ray beam is shuttered during the cardiac phase interval 0%-40% to reduce the radiation dose delivered to the patient. Only five such dose-modulated helices are sufficient to provide substantially spatially uniform sampling across the $[z_{low}, z_{high}]$ range. Moreover, the five helices provide imaging data extending across the full volume of interest (z=0 through z=120), albeit at different cardiac phases. This spatially extended imaging data can be used, for

example, to perform image registration using relatively stationary imaged features such as chest walls.

With reference to FIGURE 3E, a bi-directional or back-and-forth axial cycling is employed to provide high resolution imaging data over a diamond-shaped region **88** and lower resolution throughout the volume of interest using twelve helical scans, six in the +Z-direction and six in the -Z-direction. Each scan spans the cardiac phase range 40%-100%, and again dose modulation is preferably performed by shuttering the x-ray beam in the 0%-40% cardiac phase range. The bi-directional imaging of FIGURE 3E provides redundant projection imaging data at crossing points of the +Z-direction and the -Z-direction scans. Dotted generally horizontal lines in FIGURE 3E show suitable cardiac state images interpolated from the acquired projection views.

With continuing reference to FIGURE 1 and with further reference to FIGURE 4, increased scanning speed for another exemplary four-dimensional computed tomography imaging embodiment is obtained by using x-ray sources located at two axial positions. In the specific arrangement of FIGURE 4, x-ray beams originating from two sources **S1**, **S2** axially spaced along a line parallel to the axial or **Z**-direction direction are used. The x-ray sources **S1**, **S2** can be a plurality of conventional x-ray tubes, anodes of a multiple-anode x-ray tube, axially spaced x-ray generation positions on an axially extended anode, or the like. For each angular viewing bin, projection data is collected for x-ray beams generated by each of the sources **S1**, **S2**.

FIGURE 4 shows a two-turn helical trajectory acquired over a single 360° gantry rotation by simultaneously acquiring projection data produced by x-ray sources **S1** and **S2**. The portion of the helix acquired using the source **S1** is shown as a thick solid helical portion, while the portion of the helix

acquired using the source **S2** is shown as a thick dashed helical portion.

The x-ray sources **S1**, **S2** are axially spaced at a distance corresponding to a linear distance that the subject support **16** moves over one 360° source rotation. Hence, after a 360° gantry rotation the source **S1** is positioned at the initial position of the source **S2** with respect to the volume of interest **46**, and the helical turns acquired using each of the sources **S1** and **S2** combine to form the single two-turn helix that spans the volume of interest **46**. A single gantry rotation provides 2×360°=720° of projection data for the two-turn helix since data is simultaneously acquired using two x-ray sources **S1** and **S2**.

Since the two-turn helix corresponds to 720° of projection data in a single gantry rotation, the acquisition rate is effectively doubled. By adding additional sources spaced 360° apart, the acquisition rate can similarly be tripled, quadrupled, etc. by using three, four, etc. cooperating sources. For example, with four sources spaced at 360° intervals, a single gantry rotation will acquire 4×360°=1440° of angular data.

The approach of FIGURE 4 retains mechanical relative motion between the x-ray sources and the couch, and hence fast retrace of the sources after each scan is difficult. Moreover, the joining of helices at 360° intervals introduces some complexities in image reconstruction since there is a temporal discontinuity at each joining point. This causes a discontinuity in the time skewing of the combined helix.

With reference to FIGURES 5A and 5B, in an electronic embodiment the x-ray source **12** preferably includes a cylindrical anode **92** aligned along the axial or **Z**-direction that rotates **94**. Other axially extended anode configurations can also be used. One or more electron accelerators $\mathbf{96_1}$, $\mathbf{96_2}$

produce one or more generally collimated electron beams that passes through an electrostatic beam deflector. The beam deflector includes electrostatic electrode elements **98, 100** coupled to the electron accelerators **96_1, 96_2**, respectively, which selectively axially deflect the electron beams. Instead of electrostatic beam deflectors, electromagnetic beam deflectors can be used.

A switch/sweep electronic controller **102** selectively switches between several selected electron beam trajectories **110, 112, 114, 116**. Each of the electron beam trajectories **110, 112, 114, 116** strike the cylindrical anode **92** at predetermined axial locations to selectively produce one of several axially spaced conical- or wedge-shaped x-ray beams **120, 122, 124, 126**. The switch/sweep electronic controller **102** additionally sweeps or shifts the electron beam trajectories **110, 112, 114, 116** axially across the anode (indicated by solid horizontal arrows in FIGURES 5A and 5B). The axial sweeping is substituted for axial movement of the subject support **16** which is used in conventional computed tomography imaging. The sweeping can be bi-directional (i.e., back-and-forth). Alternatively, a sweep in one direction (indicated by the solid horizontal arrows) is followed by a fast re-trace (indicated by dashed horizontal arrows in FIGURES 5A and 5B).

The rotation **94** distributes heat generation across a surface of the anode **92**. Preferably, the cylindrical anode **92** is also actively cooled using water or another coolant fluid. The coolant fluid can be delivered into the cylindrical anode **92** (which is hollow in this internally cooled arrangement) or thermally coupled to the cylindrical anode **92** by hollow coolant lines, structures, or other shrouding disposed nearby. For example, a shroud **128** which receives coolant is disposed adjacent but displaced from the anode on a side opposite the side struck by the electron beam, and extends partially around

the cylindrical anode. Preferably, the electron beams **110, 112, 114, 116** strike the cylindrical anode **92** at about a 45° angle relative to a surface normal of the anode **92**. Thermal management is further enhanced by sweeping the beams **110, 112, 114, 116** across the anode **92**.

Of course, greater or fewer than four x-ray beams can be generated along the cylindrical anode **92**, limited by the electron beam spot size, an axial length of the cylindrical anode **92**, and the like. The wedge-shaped x-ray beams **120, 122, 124, 126** should have widths such that they do not overlap at the x-ray detector **20**, and this presents a further limitation on the number of beams. The x-ray tube **12** preferably can produce different numbers and axial spacings of x-ray beams and different beam sweep rates by selective configuring of the switch/sweep electronic controller **102**. In one preferred embodiment, the cylindrical anode **92** has an axial length of about fifteen centimeters which corresponds to a length of a typical heart in the axial direction plus cone beam fan.

In one suitable exemplary arrangement, four x-ray beams **120, 122, 124, 126** are generated as shown in FIGURES 5A and 5B. The x-ray beams **120, 122** are generated by the first electron accelerator $\mathbf{96_1}$. The x-ray beams **124, 126** are generated by the second electron accelerator $\mathbf{96_2}$. The x-ray beams **120, 124** are generated together as shown in FIGURE 5B. Collimators **130** restrict the x-ray beams **120, 124** to avoid overlap at the detector **20**. Similarly, the x-ray beams **122, 126** are generated together as indicated in phantom in FIGURE 5B. Collimators **130** restrict the x-ray beams **122, 126** to avoid overlap at the detector **20**. Hence, the x-ray tube **12** in cooperation with the collimators **130** can alternate between the x-ray beams **120, 124** and the x-ray beams **122, 126** in alternating projection views, and so projection data can be acquired along two interlaced helices as the gantry rotates.

With continuing reference to FIGURES 1, 5A, and 5B, and with further reference to FIGURES 6A, 6B, and 7, the x-ray tube **12** provides for acquisition of two helices, namely helix **I** and helix **II**. In FIGURES 6A and 6B, portions of the helices lying in front of the region of interest **46** are represented by solid lines, while helix portions that pass behind the region of interest **46** are represented by dotted lines.

Trajectories of x-ray beams **120, 122, 124, 126** during gantry **18** rotation between 0° and 180° are shown in FIGURE 6A. Trajectories of x-ray beams **120, 122, 124, 126** during gantry **18** rotation between 180° to 360° are shown in FIGURE 6B. The anode **92** and a starting emission position for each of the x-ray beams **120, 122, 124, 126** on the anode **92** (the latter designated by open circles in FIGURES 6A and 6B) are indicated in phantom using thin dashed lines in FIGURES 6A and 6B. The x-ray beams **120, 122, 124, 126** sweep together across the anode **92**.

FIGURE 7 shows a plot of x-ray beam position (relative to the starting emission position) versus the gantry angular position. Moreover, for each of the labeled gantry positions 0°, 90°, 180°, 270°, 360°, a schematic representation of the position of the anode **92** with the x-ray beam generation positions relative to the volume of interest **46** is shown below the gantry angular label.

Unlike the previous embodiments, the electronic embodiment of FIGURES 6A, 6B, and 7 does not employ linear movement of the subject support **16** during the imaging. Rather, helical source trajectories are achieved by axially scanning the x-ray-generating electron beam paths **110, 112, 114, 116** along the anode **92** during rotation of the gantry **18**. Each electron beam path **110, 112, 114, 116** moves from the starting emission position (indicated by the open circle) a distance P/2 between 0° and 180°, where P is the axial length of a full 360° turn of the helix. Correspondingly, each x-ray beam **120, 122,**

124, **126** moves along a half-turn **140** of a helix of axial length P during the first 180° of rotation. The x-ray beams **120**, **124** produce two half-turns **140** corresponding to helix **I**. The x-ray beams **122**, **126** produce two half-turns **140** corresponding to helix **II**.

In a suitable timing sequence, in a first angular view the x-ray beams **120**, **124** are operating to generate projection data for the helix **I**, while the x-ray beams **122**, **126** are off. In the next adjacent angular view the x-ray beams **122**, **126** are operating to generate projection data for the helix **II**, while the x-ray beams **120**, **124** are off. As seen in FIGURE 5A, this timing is suitably implemented using the cooperating electron accelerators $\mathbf{96_1}$, $\mathbf{96_2}$ and the beam deflectors **98**, **100**. Moreover, as seen in FIGURE 5B the collimators **30** ensure that with this timing sequence there is no overlapping of operating x-ray beams.

At 180°, a fast retrace portion **142** returns the electron beams **110**, **112**, **114**, **116** to the starting emission positions indicated by open circles. Each electron beam **110**, **112**, **114**, **116** again moves from the starting emission position the distance P/2 between 180° and 360°, and correspondingly each x-ray beam **120**, **122**, **124**, **126** moves along a second half-turn **144** of the helix and combine with half-turns **140** to complete full turns. The x-ray beams **122**, **126** produce two half-turns **144** corresponding to helix **I**. The x-ray beams **120**, **124** produce two half-turns **144** corresponding to helix **II**. At 360°, a second fast retrace portion **146** again returns the electron beams **110**, **112**, **114**, **116** to the starting emission positions. The process is repeated for each 360° gantry rotation during imaging.

The fast retrace removes the temporal discontinuity at joining points of helix portions generated by different x-ray beams. However, optionally some overscan is performed to

facilitate feathering of the cone beam projection data at the joining points.

Using the two interlaced helices **I**, **II** as shown in FIGURES 6-7, the entire volume of interest **46** is scanned in a single gantry rotation. A reduced sampling interval between acquisition of image representations of the volume of interest **46** of T_{rot}/M is obtained where T_{rot} is the time for a single rotation of the gantry **18** and x-ray source **12**, and M is the number of x-ray beams. Hence, for the arrangement of FIGURES 6-7 the time interval between scans of the volume of interest **46** is $T_{rot}/4$. This results in a reduced time skew in each image representation of the volume of interest **46**.

The sampling rate for the electronic embodiment described with particular reference to FIGURES 5-7 is substantially higher than that which is achieved using the mechanical embodiments of FIGURES 2-4. However, each of helix **I** and helix **II** will have some time skew. Hence, when using the electronic embodiment of FIGURES 5-7, the average voxel acquisition time values given in equations (3) and (4) are preferably computed by the voxel time processor **66** for each voxel of each reconstructed image. The voxel interpolator **68** suitably applies interpolation, curve fitting, or the like to determine a time-dependent value for each voxel in the region of interest **46**.

Each voxel is sampled two times per gantry rotation: once by helix **I**, and once by helix **II**. For a rotation rate of, for example, 150 rpm, this means that each voxel is sampled every 200 milliseconds. For a heart rate of 75 beats per minute, the cardiac cycle period is 800 milliseconds, and so each voxel is sampled four times per cardiac cycle.

With reference to FIGURE 8A, voxel acquisition times for voxels lying on the central cylindrical axis **48** of the volume of interest **46** is shown. Data acquired using the x-ray

beam **120** is shown by solid lines, data acquired using the x-ray beam **122** is shown by long dashed lines, data acquired using the x-ray beam **124** is shown by short dashed lines, and data acquired using the x-ray beam **126** is shown by dotted lines. For a 150 rpm gantry rotation the acquisition sequence of FIGURE 8A samples each voxel every 200 milliseconds. In one data processing approach, voxel values are interpolated for times at 100 millisecond increments, as indicated by thin dotted horizontal lines. This provides eight samples per cardiac cycle for a heart rate of 75 beats per minute. The interpolated data provides a four-dimensional data set from which can be extracted anatomical portions at selected cardiac states or phases.

For the same timing as shown in FIGURE 8A except at a rotation of 300 rpm, each voxel is sampled every 100 milliseconds, enabling interpolation at 50 millisecond increments to provide sixteen interpolated samples per cardiac cycle for a heart rate of 75 beats per minute. Because of this large number of samples per cardiac cycle, the imaging illustrated in FIGURE 8A is optionally performed without cardiac gating via the electrocardiograph **30**. Rather, the computed tomography images are acquired rapidly enough to provide interpolated cardiac phase resolution from which cardiac cycling information can be directly extracted. This direct approach is particularly beneficial for diagnosing an arrhythmic heart in which the cardiac cycle varies rapidly from heart beat to heart beat.

With reference to FIGURE 8B, another imaging session is simulated, which employs the electronic embodiment of FIGURES 5-7 with cardiac gating and a 300 rpm gantry rotation. The four x-ray beams **120, 122, 124, 126** are swept forward twice for one phase, e.g. at end-systole, at around 200 milliseconds in exemplary FIGURE 8B. The four x-ray beams **120, 122, 124, 126**

are swept backward twice for a corresponding phase of diastasis, at around 600 milliseconds in exemplary FIGURE 8B for a heart rate of about 75 beats per minute.

With returning reference to FIGURE 5A and 5B, the x-ray tube **12** which includes the elongated cylindrical anode **92** is particularly suitable for switched/sweeping beam imaging modes such as are described with reference to FIGURES 6-8. However, the x-ray tube **12** of FIGURES 5A and 5B can also perform conventional single-spot computed tomography by omitting switching of the electron beam along the cylindrical anode **92**. Hence, for example, the single-spot imaging trajectories shown in FIGURE 2 can be acquired using the x-ray tube **12** of FIGURE 5 by configuring the controller **102** to produce a single unswitched x-ray beam. However, in such a single-beam mode the anode **92** can be substantially heated at the fixed x-ray generation spot. Hence, for the single-spot imaging trajectories shown in FIGURE 2 a conventional x-ray tube may be preferable.

Similarly, the x-ray tube **12** of FIGURE 5 can be used to perform a single helical scan over one or more gantry rotations by sweeping a single electron beam axially across the anode **92**. Hence, conventional helical conebeam computed tomography imaging can be performed using the x-ray tube **12** without linear motion of the subject support **16**.

Having thus described the preferred embodiments, the invention is now claimed to be:

1. A helical cone beam computed tomography imaging method comprising:

acquiring helical cone beam computed tomography projection data for a volume of interest (46) using a plurality of source trajectory helices;

reconstructing the acquired helical cone beam computed tomography projection data for each helix to generate a corresponding time skewed volume image representation of the volume of interest (46);

for each time skewed volume image representation, computing a voxel acquisition time for each voxel; and

for each voxel, computing an interpolated voxel value based on values of the voxel in the plurality of image representations and corresponding voxel acquisition times.

2. The imaging method as set forth in claim 1, wherein the time skewed volume image representations temporally overlap.

3. The imaging method as set forth in either one of claim 1 and claim 2, wherein time intervals between voxel acquisition times for at least some voxels are less than a time interval over which a helix is acquired.

4. The imaging method as set forth in any one of claims 1-3, wherein the volume of interest (46) undergoes a cyclical temporal variation, and each source trajectory helix spans the volume of interest (46) over a time interval less than one cycle period of the cyclical temporal variation of the volume of interest (46).

5. The imaging method as set forth in any one of claims 1-4, wherein the reconstructing of the acquired helical cone beam computed tomography projection data for each helix to generate a corresponding time skewed volume image representation of the volume of interest (46) includes:

for each voxel, reconstructing a temporally contiguous projection data set corresponding to the voxel, the temporally contiguous projection data set having been acquired over a single contiguous acquisition time interval within the corresponding source trajectory helix.

6. The imaging method as set forth in claim 5, wherein the computing of a voxel acquisition time for each voxel of each time skewed volume image representation includes:

computing the voxel acquisition time as a time average of the contiguous acquisition time interval corresponding to the voxel.

7. The imaging method as set forth in either one of claim 5 and claim 6, wherein the computing of a voxel acquisition time for each voxel of each time skewed volume image representation includes:

identifying a PI line associated with the voxel;

determining a PI line time interval corresponding to the PI line; and

computing the voxel acquisition time as a statistical characteristic time value of the PI line time interval.

8. The imaging method as set forth in any one of claims 1-7, wherein the acquiring of helical cone beam computed tomography projection data for a volume of interest (46) using a plurality of source trajectory helices includes:

for each helix, acquiring generally non-overlapping projection views during adjacent helical turns.

9. The imaging method as set forth in any one of claims 1-8, wherein at least some of the plurality of source trajectory helices span less than the entire volume of interest (46).

10. The imaging method as set forth in any one of claims 1-9, wherein the acquiring of helical cone beam computed tomography projection data for a volume of interest (46) using a plurality of source trajectory helices includes:

rotating a radiation source (12) about the volume of interest (46); and

simultaneously with the rotating, cyclically relatively axially moving the volume of interest (46) and the radiation source (12).

11. The imaging method as set forth in claim 10, wherein the acquiring of helical cone beam computed tomography projection data for a volume of interest (46) using a plurality of source trajectory helices includes:

during the simultaneous rotating and relative axial moving, acquiring projection data using a plurality of axially spaced radiation cone beam source positions.

12. The imaging method as set forth in any one of claims 1-9, wherein the acquiring of helical cone beam computed tomography projection data for a volume of interest (46) using a plurality of source trajectory helices includes:

rotating a cone beam radiation source (12) about the volume of interest (46); and

simultaneously with the rotating, axially sweeping an electron beam across an axially elongated anode (92) of the radiation source (12), the electron beam defining an x-ray cone beam generation position on the anode (92), the rotating and

the axial sweeping cooperating to generate the source trajectory helices.

13. The imaging method as set forth in claim **12**, wherein the acquiring of helical cone beam computed tomography projection data for a volume of interest **(46)** using a plurality of source trajectory helices further includes:

fast re-tracing the axial sweep between source trajectory helices.

14. The imaging method as set forth in either one of claim **12** and claim **13**, wherein the axial sweeping includes simultaneously axially sweeping at least two x-ray cone beam generation positions across the axially elongated anode **(92)**.

15. The imaging method as set forth in any one of claims **1-14**, wherein the volume of interest **(46)** includes a cardiac region and the acquiring of helical cone beam computed tomography projection data for the volume of interest **(46)** using a plurality of source trajectory helices includes:

triggering each source trajectory helix based on detection of a selected cardiac phase.

16. The imaging method as set forth in claim **15**, wherein the selected triggering cardiac phase is different for each helix.

17. The imaging method as set forth in either one of claim **15** and claim **16**, wherein at least two source trajectory helices are triggered within a single cardiac cycle.

18. The imaging method as set forth in any one of claims **1-17**, wherein the volume of interest **(46)** includes a cyclically temporally varying organ and the computing of an interpolated voxel value includes:

interpolating voxels of the time skewed volume image representations that have voxel acquisition times corresponding to a selected state of the cyclically temporally varying organ.

19. The imaging method as set forth in any one of claims **1-18**, wherein the computing of an interpolated voxel value includes:

for each voxel, computing a time-dependent voxel value based on values of the voxel in the plurality of time skewed volume image representations and corresponding voxel acquisition times.

20. An apparatus for performing helical cone beam computed tomography imaging, the apparatus comprising:

a means **(10)** for acquiring helical cone beam computed tomography projection data for a volume of interest **(46)** using a plurality of source trajectory helices;

a means **(62)** for reconstructing the acquired helical cone beam computed tomography projection data for each helix to generate a corresponding time skewed volume image representation of the volume of interest **(46)**;

a means **(66)** for computing a voxel acquisition time for each voxel of each time skewed image representation; and

a means **(68)** for computing an interpolated voxel value for each voxel based on values of the voxel in the plurality of time skewed image representations and corresponding voxel acquisition times.

21. The apparatus as set forth in claim **20**, wherein the volume of interest **(46)** includes at least a portion of the heart, and the means **(10)** for acquiring helical cone beam computed tomography projection data for a volume of interest **(46)** using a plurality of source trajectory helices includes:

an electrocardiograph (30) that triggers the source trajectory helices.

22. The apparatus as set forth in claim 21, wherein the means (68) for computing an interpolated voxel value includes:

a means for selecting voxel values from the time skewed volume image representations whose corresponding voxel acquisition times correspond to an occurrence of one of a selected cardiac phase and a selected state of cardiac motion; and

a means for combining the selected voxel values to generate an image representation of the selected cardiac phase or selected state of cardiac motion.

23. The apparatus as set forth in any one of claims 20-22, wherein the means (68) for computing an interpolated voxel value for each voxel includes:

a means for computing a time-dependent voxel value based on the values of the voxel in the plurality of time skewed volume image representations and corresponding voxel acquisition times.

24. The apparatus as set forth in any one of claims 20-23, wherein the means (10) for acquiring helical cone beam computed tomography projection data includes:

a rotating gantry (18);

an x-ray source (12) arranged on the rotating gantry (18), the x-ray source (12) including an axially extended anode (92) and an electron source (96_1, 96_2) that axially sweeps an electron beam along the anode (92) to produce an axially sweeping x-ray cone beam, the axial sweeping cooperating with rotating of the gantry (18) to produce the source trajectory helices;

a radiation detector (20) arranged to detect x-rays produced by the x-ray source (12) after passing through the volume of interest (46); and

a support structure (16) that supports an imaging subject, at least a portion of which imaging subject defines the volume of interest (46).

25. The apparatus as set forth in claim 24, further including:

a beam-switching means (102) for switching the sweeping electron beam between a plurality of axially spaced positions on the anode (92) to produce a plurality of axially spaced sweeping x-ray cone beams (120, 122, 124, 126).

26. The apparatus as set forth in any one of claims 20-23, wherein the means (10) for acquiring helical cone beam computed tomography projection data includes:

a rotating gantry (18);

an x-ray source (12) arranged on the rotating gantry (18), the x-ray source (12) rotating with the rotating gantry (18) and producing an x-ray cone beam that passes through the volume of interest (46);

a radiation detector (20) arranged to detect x-rays produced by the x-ray source (12) after passing through the volume of interest (46);

a support structure (16) that supports an imaging subject, at least a portion of which imaging subject defines the volume of interest (46); and

a means (98, 100) for relatively axially moving the support structure and the x-ray cone beam, the axial moving cooperating with rotating of the gantry (18) to produce the source trajectory helices.

27. The apparatus as set forth in any one of claims 20-23, wherein the means (10) for acquiring helical cone beam computed tomography projection data includes:

a rotating gantry (18);

an x-ray source (12) disposed on the rotating gantry (18) and rotating therewith, the x-ray source (12) including an axially oriented cylindrical anode (92), an electron source (96_1, 96_2) irradiating the cylindrical anode (92) to produce an x-ray beam traversing a volume of interest, and an electron beam deflector (98, 100) that axially deflects the electron beam along the cylindrical anode (92) to axially sweep the x-ray beam, the deflector (98, 100) cooperating with the rotating gantry (18) to produce a helical trajectory of the x-ray beam about the volume of interest (46); and

a radiation detector (20) arranged to measure the x-ray beam after passing through the volume of interest (46).

28. The apparatus as set forth in claim 27, wherein the electron beam deflector (98, 100) switches the electron beam between at least two axially spaced positions on the anode (92), the at least two axially spaced positions selected to define at least two helical trajectories each spanning a portion of the volume of interest (46) and arranged to cooperatively define a helical trajectory spanning the volume of interest (46).

29. The apparatus as set forth in claim 27, wherein the electron beam deflector (98, 100) switches the electron beam between at least two axially spaced positions on the anode (92), the at least two axially spaced positions selected to define at least two interlaced helical trajectories.

30. An x-ray tube (12) comprising:

a cylindrical anode **(92)** whose cylindrical axis is axially oriented;

an electron source **(96_1, 96_2)** that produces an electron beam generally directed toward the cylindrical anode **(92)**, which electron beam interacts with the cylindrical anode **(92)** to produce x-rays; and

an electron beam deflector **(98, 100)** that sweeps the electron beam axially across the cylindrical anode **(92)**.

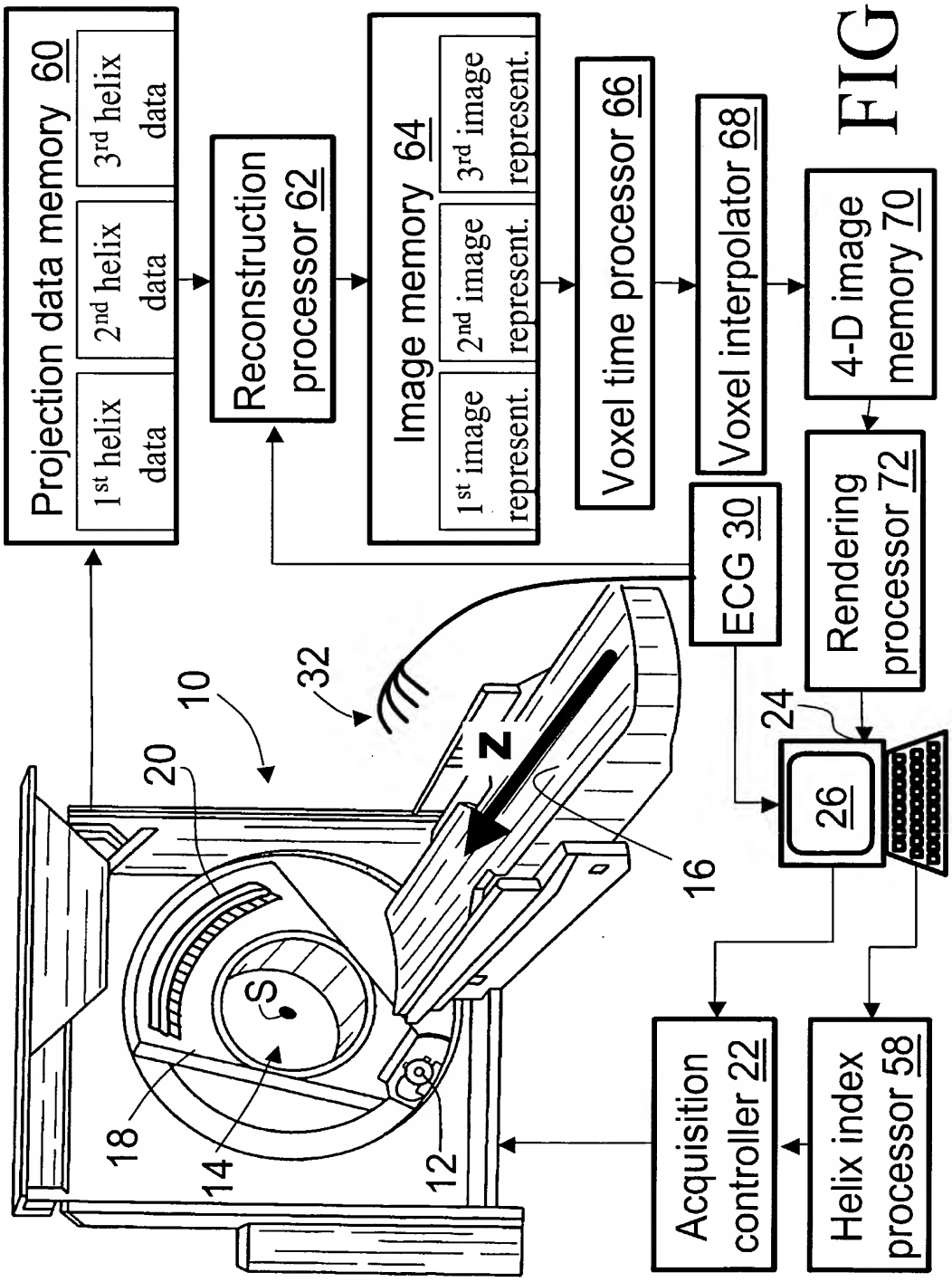
Projection data memory 60
1st helix data
2nd helix data
3rd helix data
Reconstruction processor 62
Image memory 64
1st image represent.
2nd image represent.
3rd image represent.
Voxel time processor 66
Voxel interpolator 68
4-D image memory 70
Rendering processor 72
ECG 30
26
24
Acquisition controller 22
Helix index processor 58
10
12
14
16
18
20
32
S
Z

FIG 1

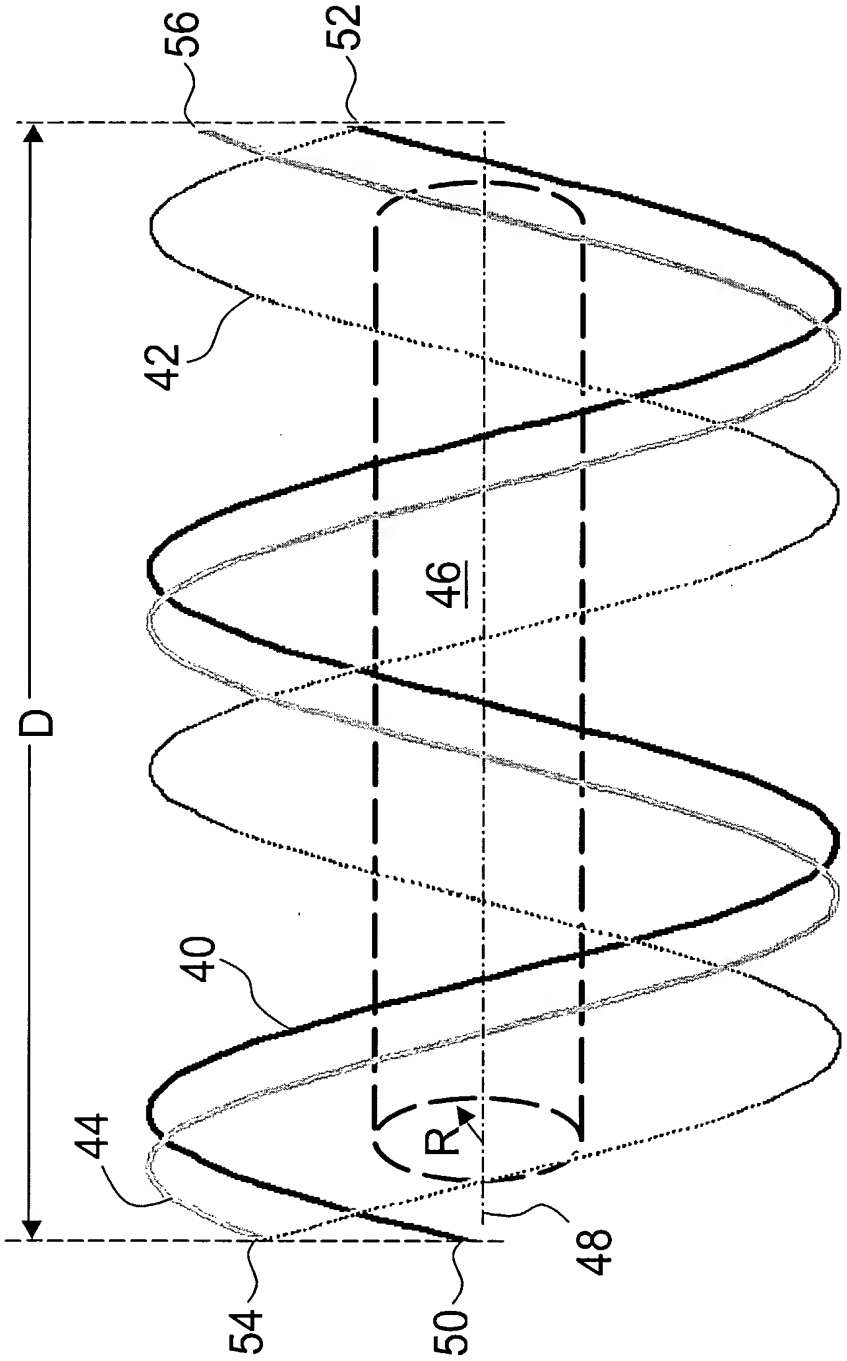

FIG 2

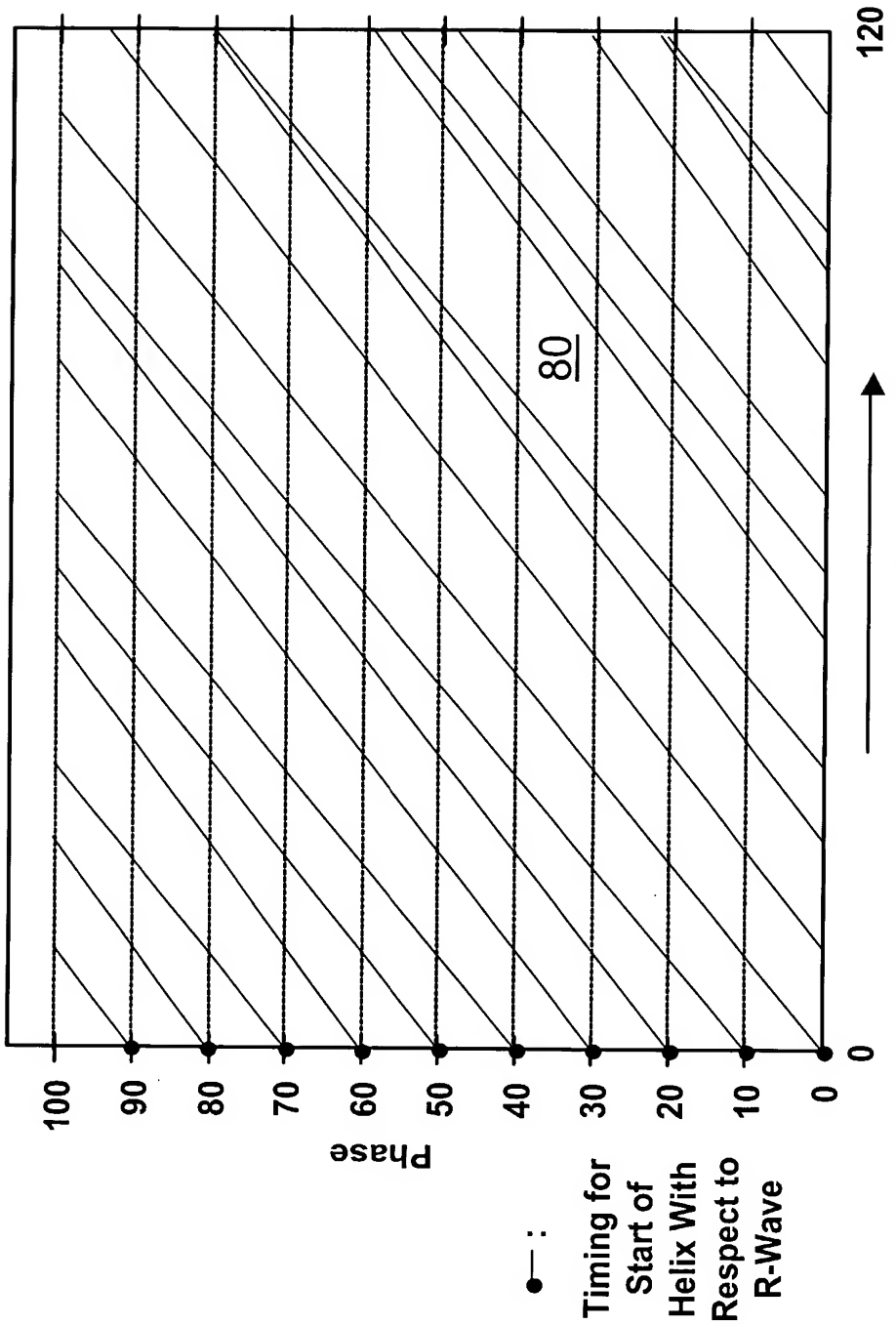
80
Timing for Start of Helix With Respect to R-Wave
Phase
100
90
80
70
60
50
40
30
20
10
0
0
120
Z (millimeters)

FIG 3A

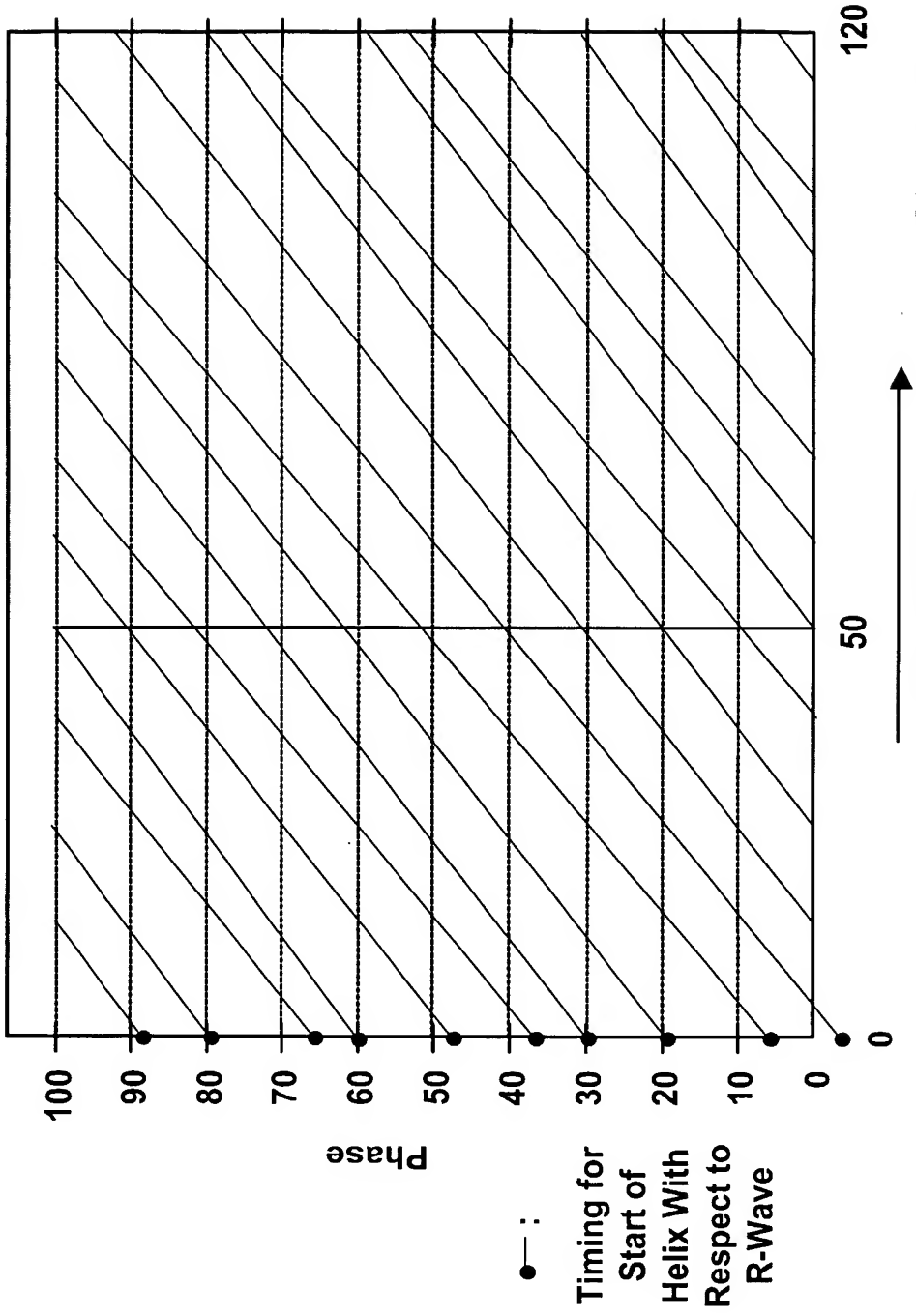
Phase
100
90
80
70
60
50
40
30
20
10
0
0
50
120
Z (millimeters)
Timing for Start of Helix With Respect to R-Wave

FIG 3B

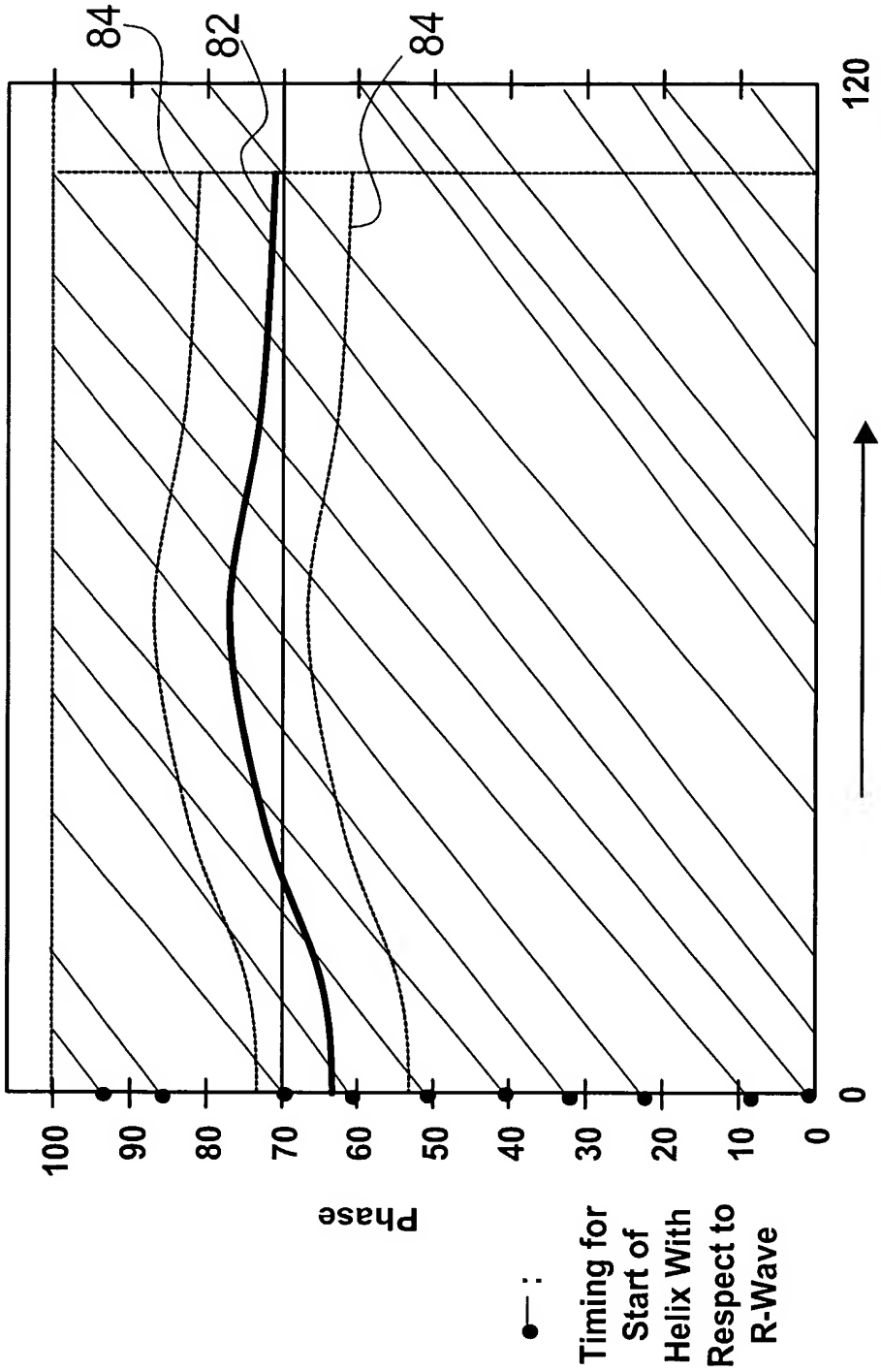
84
82
84
120
0
100
90
80
70
60
50
40
30
20
10
0
Phase
Z (millimeters)
Timing for Start of Helix With Respect to R-Wave

FIG 3C

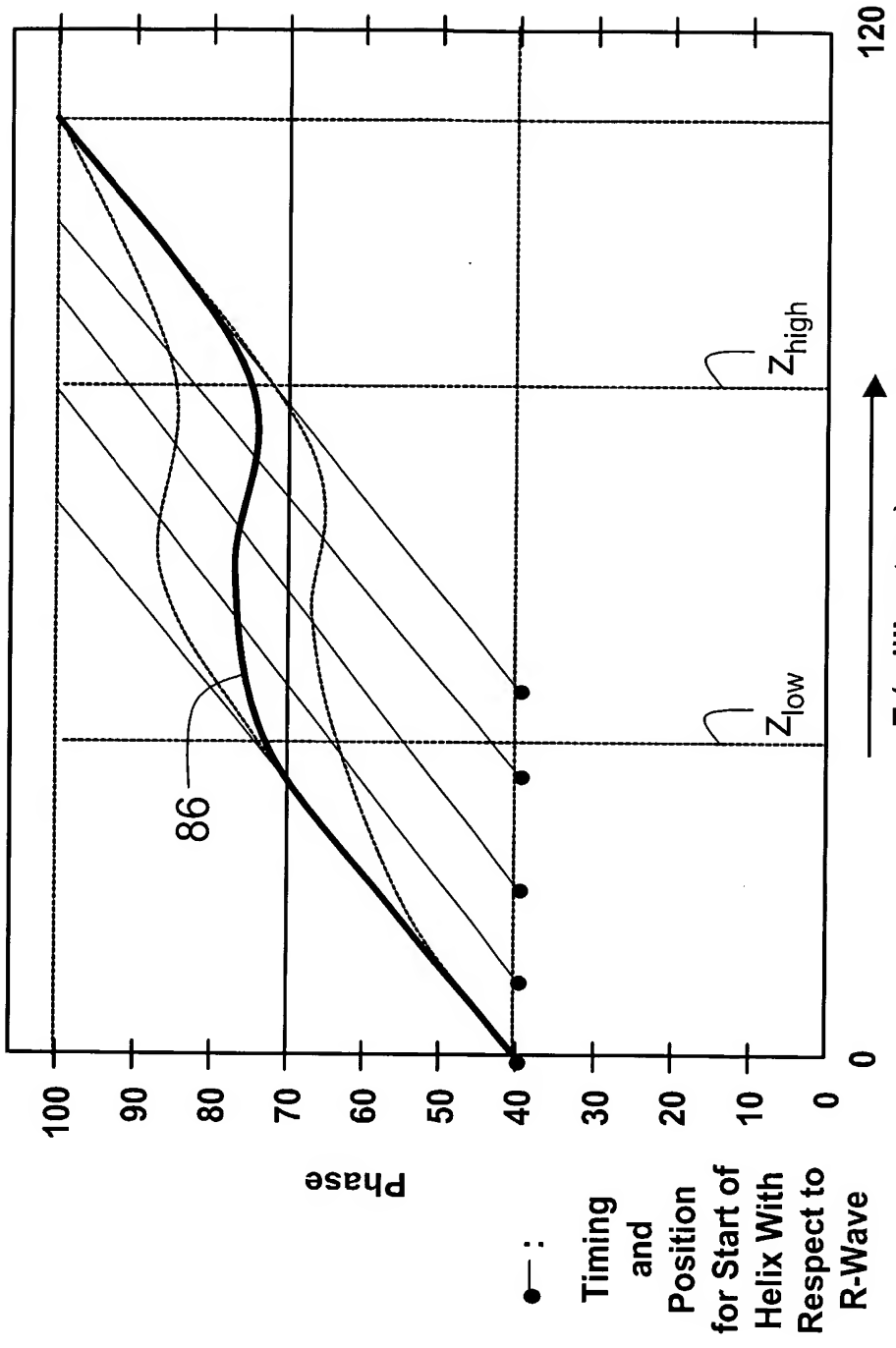
Phase
100
90
80
70
60
50
40
30
20
10
0
0
120
Z (millimeters)
Z_{high}
Z_{low}
86
Timing and Position for Start of Helix With Respect to R-Wave

FIG 3D

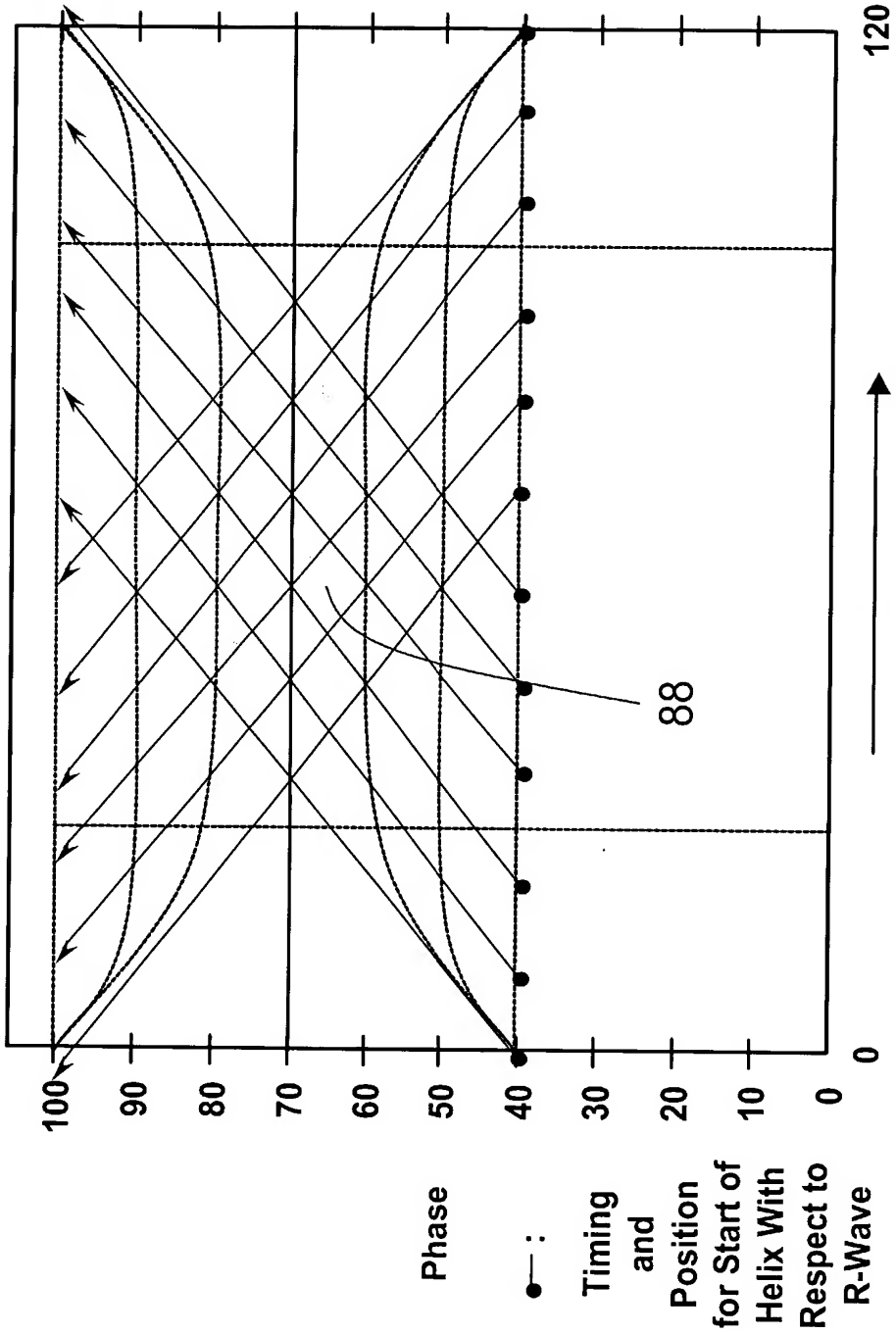
Phase
100
90
80
70
60
50
40
30
20
10
0
Timing and Position for Start of Helix With Respect to R-Wave
88
0
120
z

FIG 3E

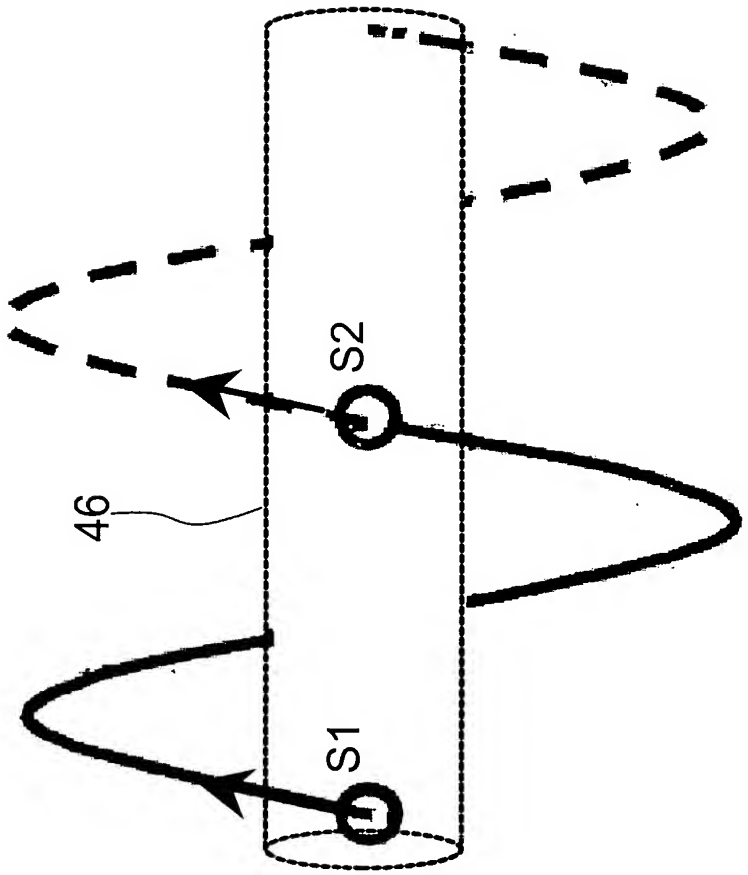

FIG 4

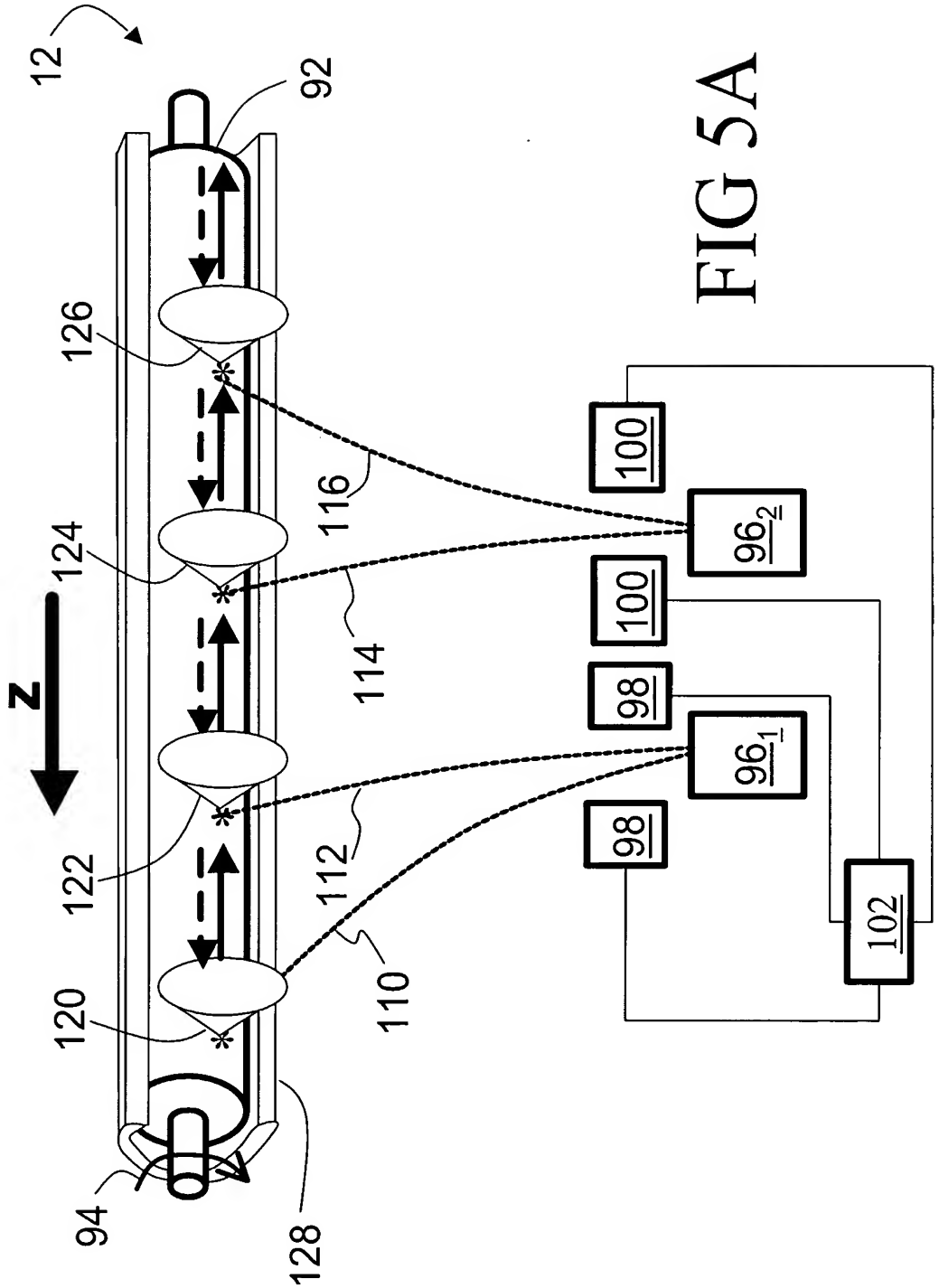
12
92
126
124
122
120
116
114
112
110
94
128
z
100
96_2
100
98
96_1
98
102

FIG 5A

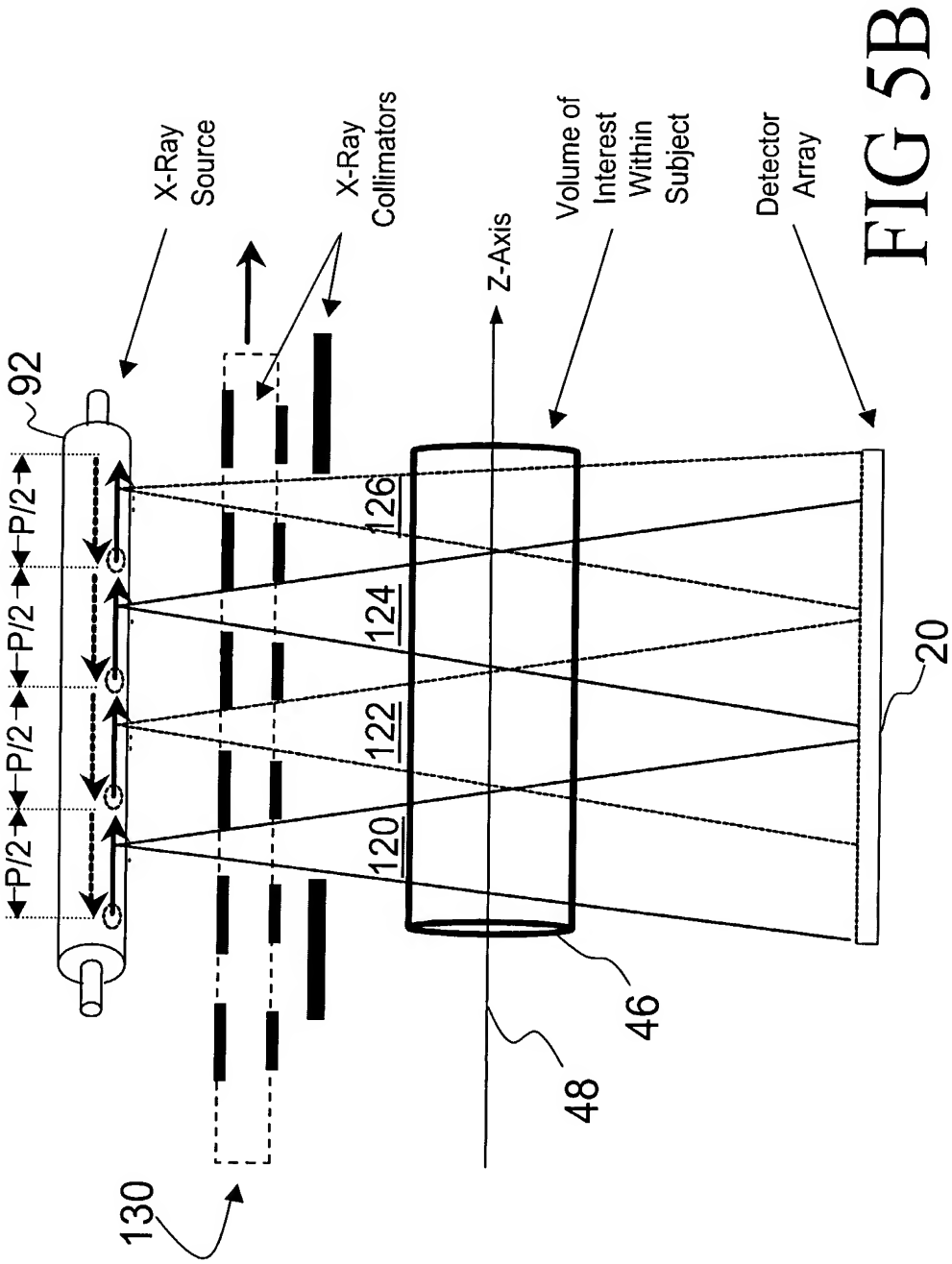
X-Ray Source
X-Ray Collimators
Z-Axis
Volume of Interest Within Subject
Detector Array
92
P/2
P/2
P/2
P/2
126
124
122
120
20
46
48
130

FIG 5B

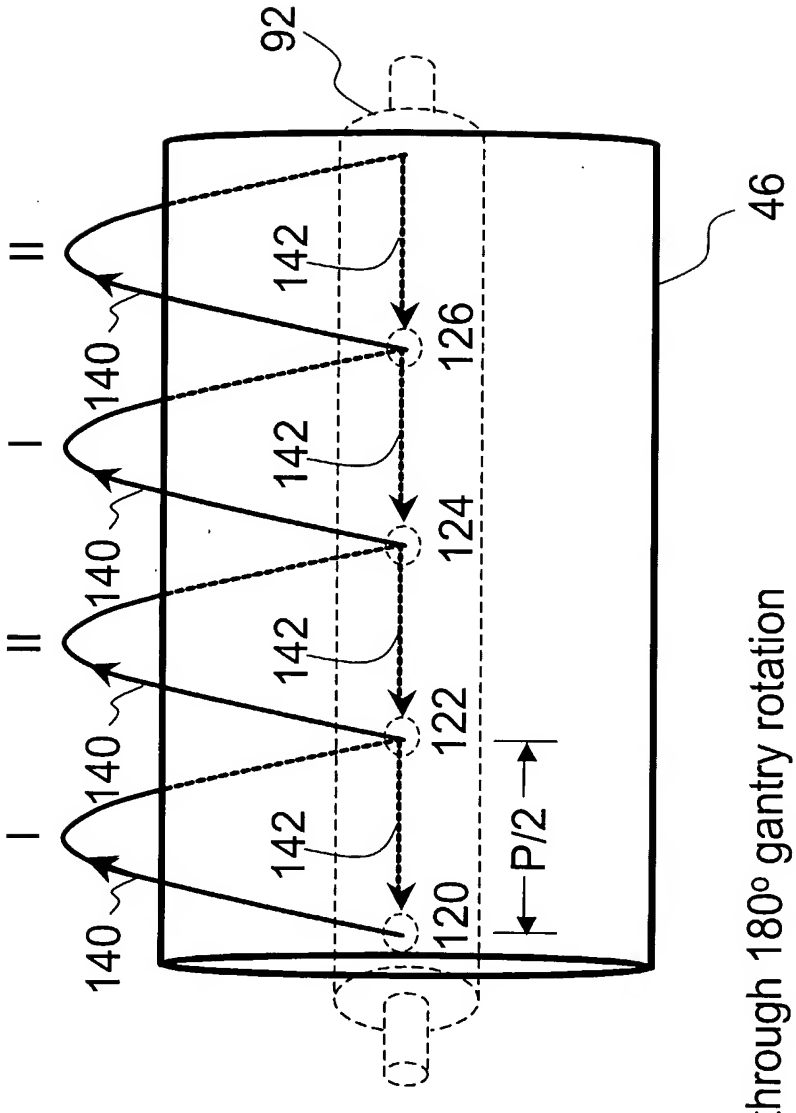
92
46
II
I
II
I
140
140
140
140
142
142
142
142
126
124
122
120
P/2
0° through 180° gantry rotation

FIG 6A

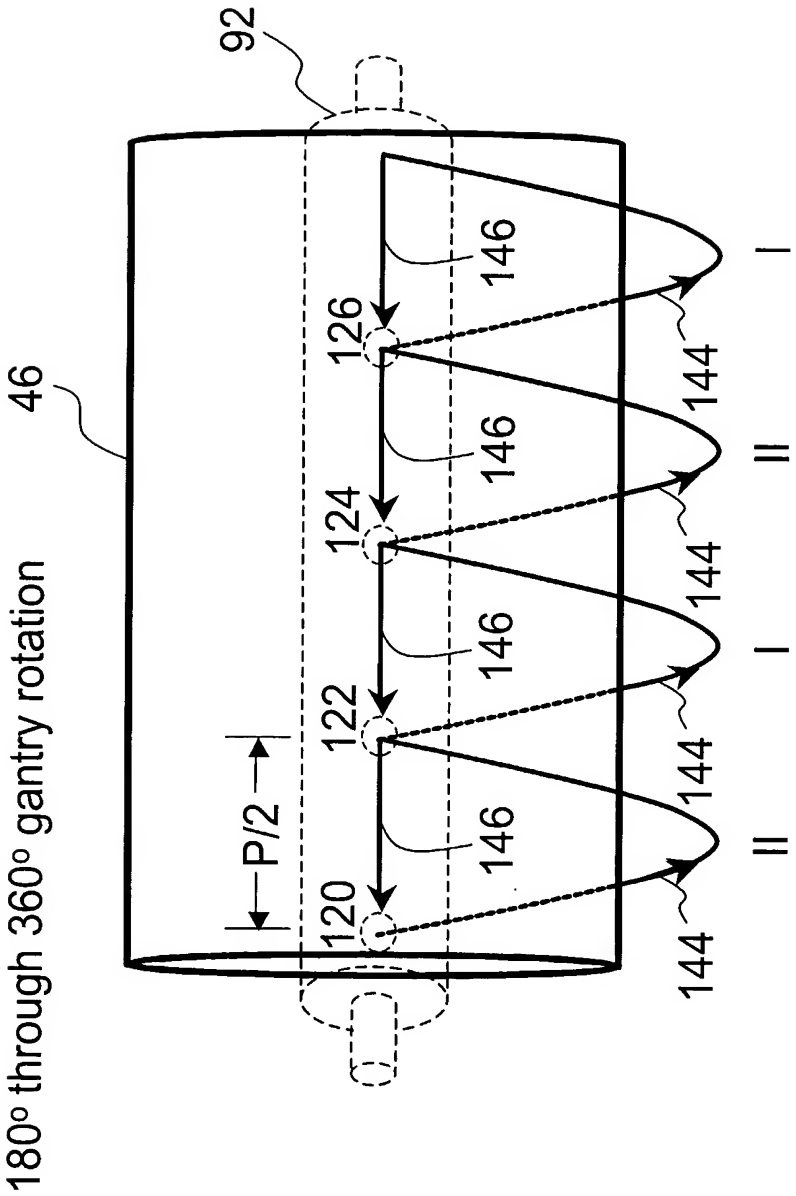
92
46
180° through 360° gantry rotation
P/2
120
122
124
126
146
144
I
II

FIG 6B

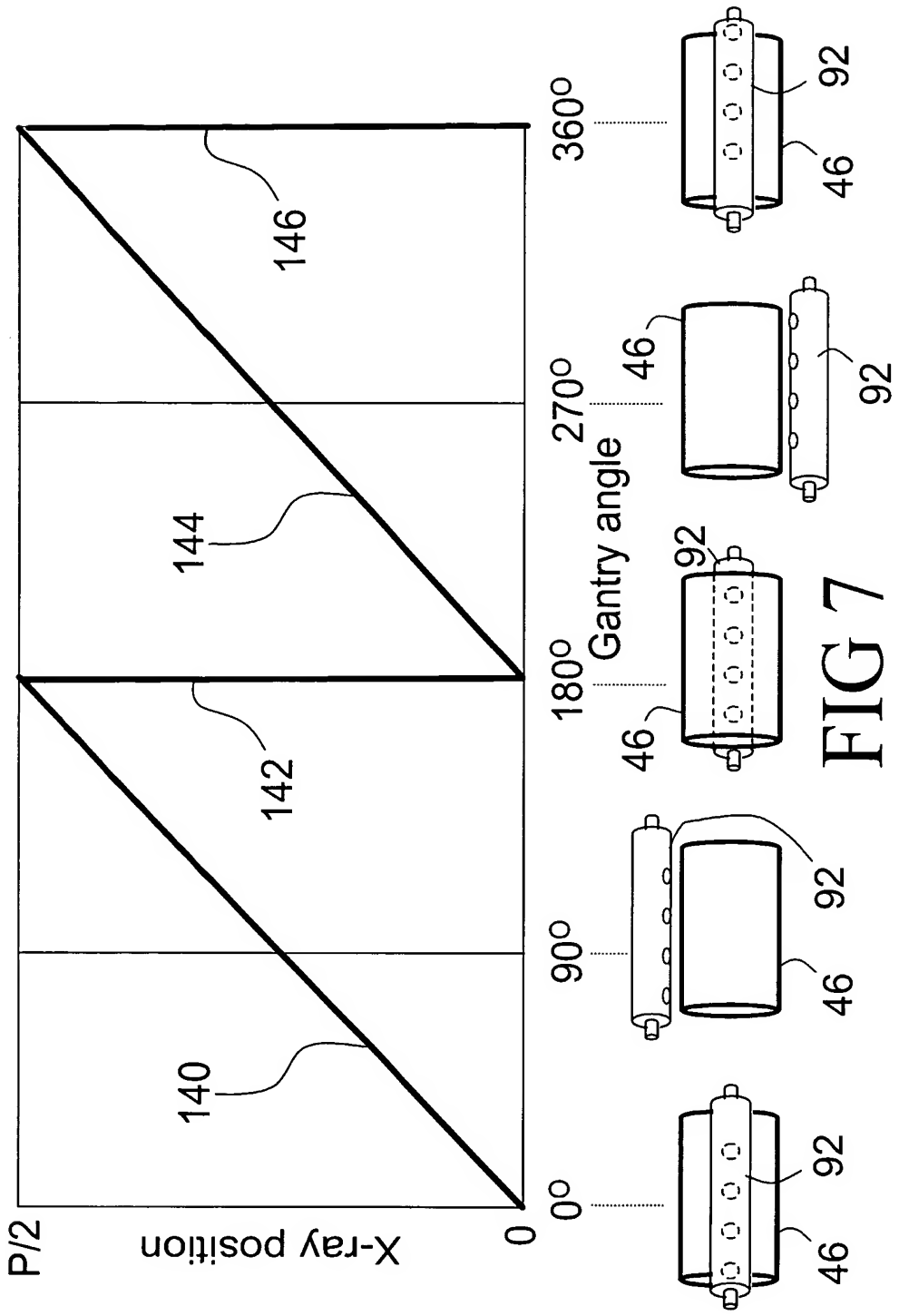
P/2
X-ray position
0
140
142
144
146
0°
90°
180°
270°
360°
Gantry angle
46
92

FIG 7

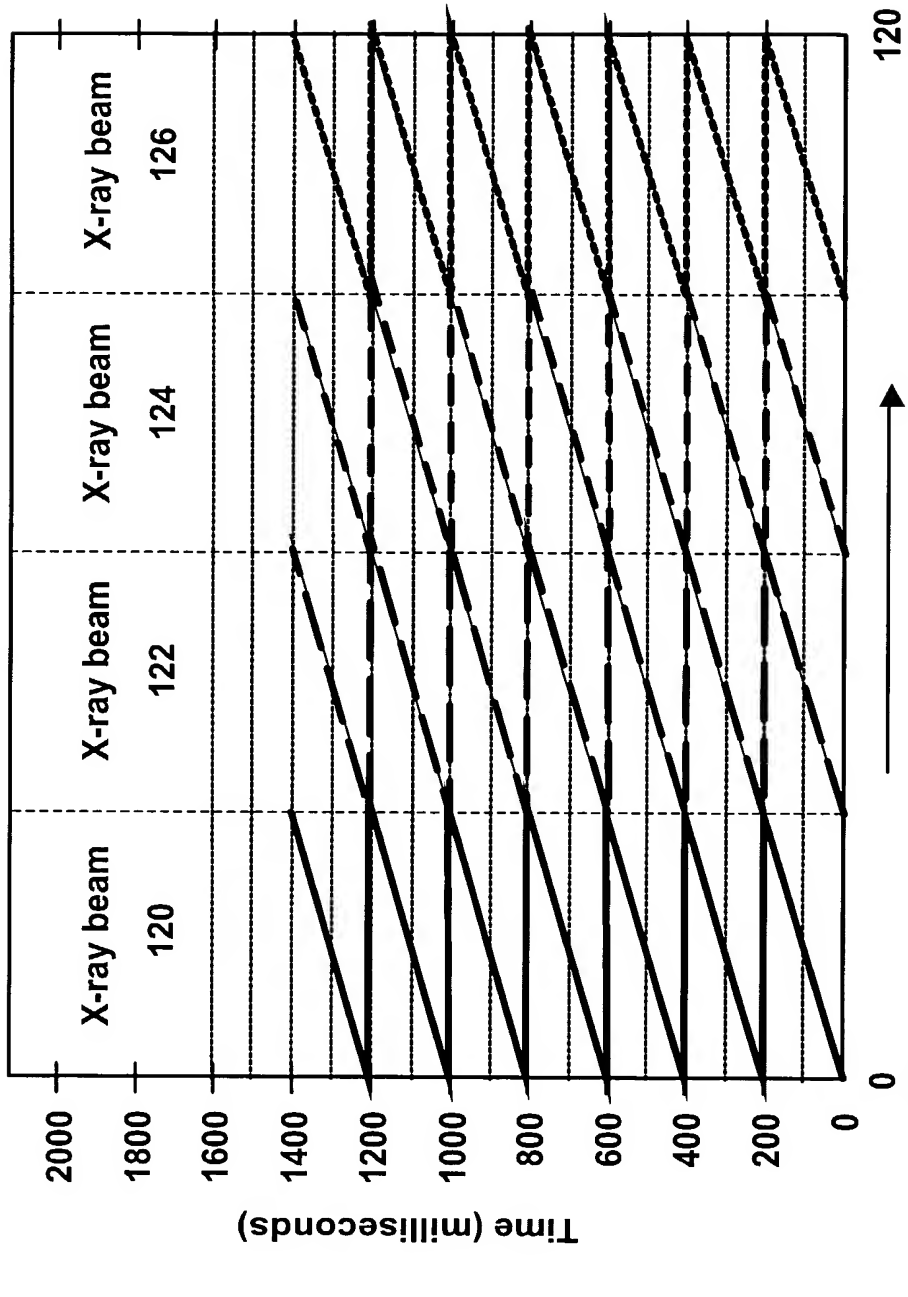
X-ray beam 120
X-ray beam 122
X-ray beam 124
X-ray beam 126
Time (milliseconds)
2000
1800
1600
1400
1200
1000
800
600
400
200
0
0
120
z (mm)
150 rpm gantry rotation
200 msec = 180° Interval

FIG 8A

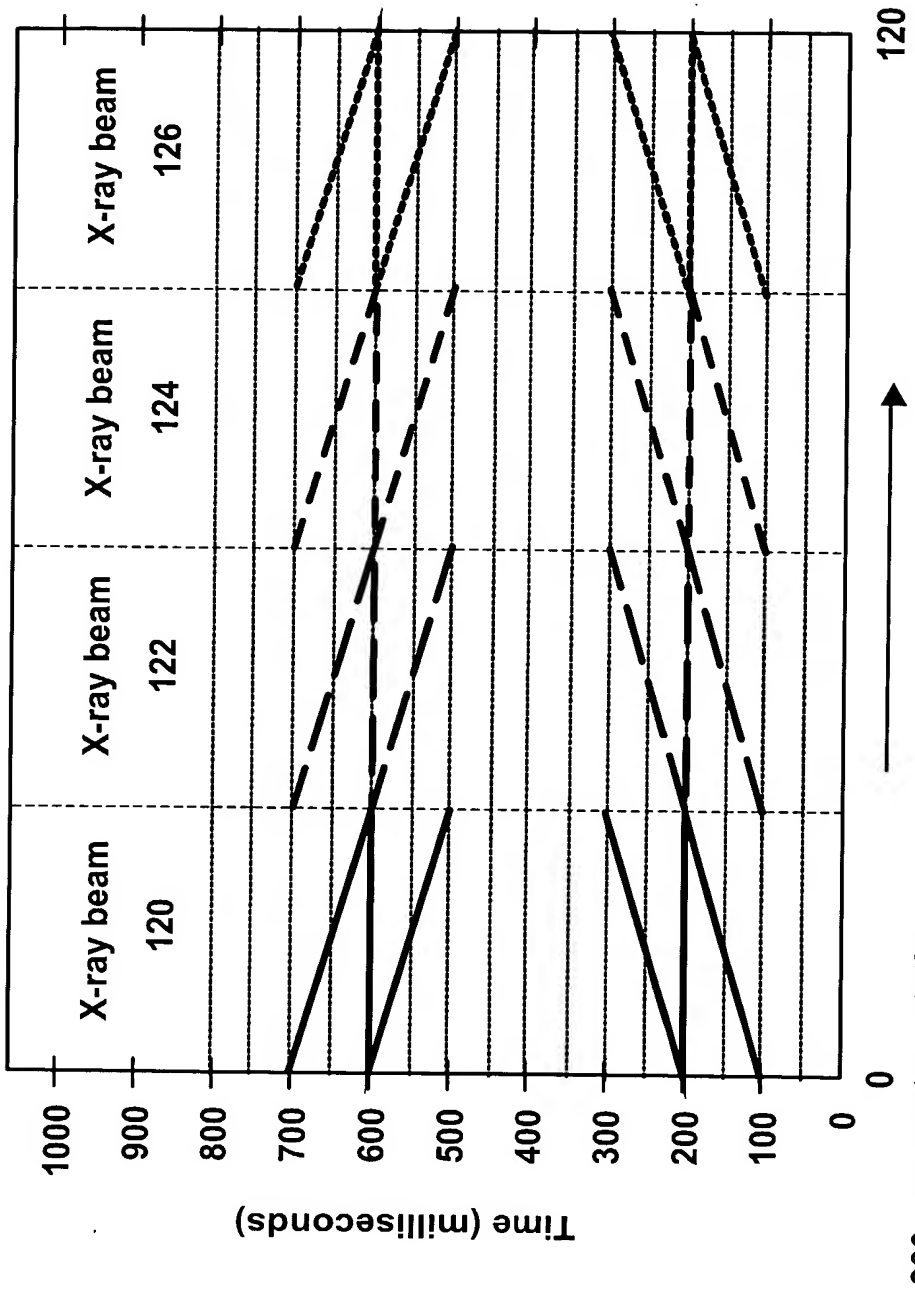
X-ray beam 120
X-ray beam 122
X-ray beam 124
X-ray beam 126
1000
900
800
700
600
500
400
300
200
100
0
Time (milliseconds)
0
120
Z (mm)
300 rpm gantry rotation
100 msec = 180° Interval

FIG 8B

INTERNATIONAL SEARCH REPORT

Interna lication No
PCT/IB 03/04457

A. CLASSIFICATION OF SUBJECT MATTER
IPC 7 A61B6/03 A61B6/00

According to International Patent Classification (IPC) or to both national classification and IPC

B. FIELDS SEARCHED

Minimum documentation searched (classification system followed by classification symbols)
IPC 7 A61B

Documentation searched other than minimum documentation to the extent that such documents are included in the fields searched

Electronic data base consulted during the international search (name of data base and, where practical, search terms used)
EPO-Internal

C. DOCUMENTS CONSIDERED TO BE RELEVANT

Category °	Citation of document, with indication, where appropriate, of the relevant passages	Relevant to claim No.
X Y	EP 0 648 468 A (PICKER INTERNATIONAL INC.) 19 April 1995 (1995-04-19) page 9, line 50 -page 10, line 2 abstract; figures 1-12	1,20 8,9,21
Y	US 5 744 802 A (MUEHLLEHNER ET AL.) 28 April 1998 (1998-04-28) column 11, line 48 -column 13, line 7; figures 1-15	8
Y	US 6 240 157 B1 (DANIELSSON) 29 May 2001 (2001-05-29) abstract; figures 1-15	9
Y	US 4 182 311 A (SEPPI ET AL.) 8 January 1980 (1980-01-08) the whole document	21

-/--

[X] Further documents are listed in the continuation of box C.

[X] Patent family members are listed in annex.

° Special categories of cited documents :

"A" document defining the general state of the art which is not considered to be of particular relevance

"E" earlier document but published on or after the international filing date

"L" document which may throw doubts on priority claim(s) or which is cited to establish the publication date of another citation or other special reason (as specified)

"O" document referring to an oral disclosure, use, exhibition or other means

"P" document published prior to the international filing date but later than the priority date claimed

"T" later document published after the international filing date or priority date and not in conflict with the application but cited to understand the principle or theory underlying the invention

"X" document of particular relevance; the claimed invention cannot be considered novel or cannot be considered to involve an inventive step when the document is taken alone

"Y" document of particular relevance; the claimed invention cannot be considered to involve an inventive step when the document is combined with one or more other such documents, such combination being obvious to a person skilled in the art.

"&" document member of the same patent family

Date of the actual completion of the international search	Date of mailing of the international search report
13 January 2004	20/01/2004

Name and mailing address of the ISA	Authorized officer
European Patent Office, P.B. 5818 Patentlaan 2 NL – 2280 HV Rijswijk Tel. (+31-70) 340-2040, Tx. 31 651 epo nl, Fax: (+31-70) 340-3016	Hunt, B

Form PCT/ISA/210 (second sheet) (July 1992)

INTERNATIONAL SEARCH REPORT

Interna ilication No
PCT/ID 03/04457

C.(Continuation) DOCUMENTS CONSIDERED TO BE RELEVANT

Category °	Citation of document, with indication,where appropriate, of the relevant passages	Relevant to claim No.
A	WO 99 018854 A (ANALOGIC CORP.) 22 April 1999 (1999-04-22) the whole document ---	1-20
A	US 2001/048731 A1 (NAKAMURA ET AL.) 6 December 2001 (2001-12-06) paragraphs '0095!-'0101! paragraphs '0133!-'0135!; figures 1-7 ---	1,4,20
A	US 5 960 056 A (LAI) 28 September 1999 (1999-09-28) the whole document ---	1,20
A	US 4 039 807 A (BULL) 2 August 1977 (1977-08-02) the whole document -----	30

INTERNATIONAL SEARCH REPORT

Interr plication No
PCT/IB 03/04457

Patent document cited in search report	Publication date	Patent family member(s)	Publication date
EP 648468 A	19-04-1995	US 5396418 A	07-03-1995
		DE 69417140 D1	22-04-1999
		DE 69417140 T2	16-09-1999
		EP 0648468 A1	19-04-1995
		JP 7178079 A	18-07-1995
		US 5485493 A	16-01-1996
		US 5544212 A	06-08-1996
US 5744802 A	28-04-1998	AU 7523796 A	15-05-1997
		DE 19681626 T0	26-11-1998
		JP 11514446 T	07-12-1999
		WO 9715841 A1	01-05-1997
US 6240157 B1	29-05-2001	EP 0892966 A1	27-01-1999
		WO 9830980 A1	16-07-1998
		CN 1258365 T	28-06-2000
		DE 59902252 D1	12-09-2002
		EP 1000408 A1	17-05-2000
		WO 9936885 A1	22-07-1999
		JP 11253434 A	21-09-1999
		JP 2001516268 T	25-09-2001
		US 6275561 B1	14-08-2001
US 4182311 A	08-01-1980	NONE	
WO 99018854 A	22-04-1999	US 5909477 A	01-06-1999
		US 5881122 A	09-03-1999
		US 5887047 A	23-03-1999
		AU 9474398 A	03-05-1999
		CN 1336811 T	20-02-2002
		EP 1021128 A1	26-07-2000
		JP 2001519192 T	23-10-2001
		WO 9918854 A1	22-04-1999
US 2001048731 A1	06-12-2001	JP 3442346 B2	02-09-2003
		JP 2001340330 A	11-12-2001
US 5960056 A	28-09-1999	AU 8274098 A	25-01-1999
		CN 1268035 T	27-09-2000
		EP 0996361 A1	03-05-2000
		JP 2001510384 T	31-07-2001
		WO 9901067 A1	14-01-1999
		AU 7959798 A	25-01-1999
		AU 8065898 A	25-01-1999
		CN 1309548 T	22-08-2001
		CN 1268034 T	27-09-2000
		EP 1005631 A2	07-06-2000
		EP 0998219 A1	10-05-2000
		JP 2001509400 T	24-07-2001
		JP 2003524430 T	19-08-2003
		TW 381012 B	01-02-2000
		US 5907594 A	25-05-1999
		US 6118841 A	12-09-2000
		WO 9901736 A2	14-01-1999
		WO 9901065 A1	14-01-1999
US 4039807 A	02-08-1977	GB 1547964 A	04-07-1979
		DE 2631516 A1	20-01-1977

INTERNATIONAL SEARCH REPORT

Inte pplication No
PCT/IB 03/04457

Patent document cited in search report	Publication date	Patent family member(s)	Publication date
US 4039807 A		FR 2317849 A1	04-02-1977
		JP 1252057 C	26-02-1985
		JP 52011791 A	28-01-1977
		JP 59027074 B	03-07-1984
		NL 7607715 A ,B,	13-01-1977